

Sulfur-Assisted Phenyl Migration from Phosphorus to Platinum in PtW₂ and PtMo₂ Clusters Containing Thioether-Functionalized Short-Bite Ligands of the Bis(diphenylphosphanyl)amine-Type

Stefano Todisco,[†] Piero Mastrorilli,^{*,†,‡} Mario Latronico,^{†,‡} Vito Gallo,[†] Ulli Englert,[§] Nazzareno Re,^{||} Francesco Creati,^{||} and Pierre Braunstein^{*,⊥}

[†]Dipartimento di Ingegneria Civile, Ambientale, del Territorio, Edile e di Chimica (DICATECh), Politecnico di Bari, via Orabona 4, I-70125 Bari, Italy

[‡]Istituto di Chimica dei Composti Organometallici (ICCOM-CNR), Consiglio Nazionale delle Ricerche, Via Orabona 4, 70125 Bari, Italy

[§]Institut für Anorganische Chemie der RWTH, Landoltweg 1, D-52074 Aachen, Germany

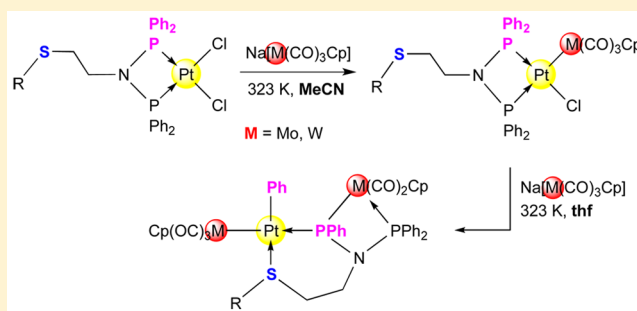
^{||}Dipartimento di Farmacia, Università G. d'Annunzio, Via dei Vestini 31, 06100 Chieti, Italy

[⊥]Laboratoire de Chimie de Coordination, UMR 7177 CNRS, Université de Strasbourg, 4 rue Blaise Pascal, CS 90032, F-67081 Strasbourg, France

Supporting Information

ABSTRACT: The reactivity of dichloroplatinum(II) complexes containing thioether-functionalized bis(diphenylphosphanyl)amines of formula (Ph₂P)₂N(CH₂)₂SR (R = (CH₂)₅CH₃, CH₂Ph) toward group 6 carbonylmetalates Na[M(CO)₃Cp] (M = Mo or W, Cp = cyclopentadienyl) was explored. Reactions with two or more equivalents of Na[M(CO)₃Cp] (M = Mo or W) afforded the trinuclear complexes of general formula [PtPh{M(CO)₃Cp}{μ-P(Ph)N(CH₂CH₂SR)(PPh₂)-κ³P,P,S}]M(CO)₂Cp (3 M = Mo, R = (CH₂)₅CH₃; 4 M = Mo, R = CH₂Ph; 9 M = W, R = (CH₂)₅CH₃; 10 M = W, R = CH₂Ph), the structure of which consists of a six-membered platinumacycle

condensed with a four-membered M–P–N–P cycle, together with small amounts of isomeric PtM₂ clusters [PtM₂(CO)₅Cp₂{(Ph₂P)₂N(CH₂CH₂SR)-κ²P,P}] (5 M = Mo, R = (CH₂)₅CH₃; 6 M = Mo, R = CH₂Ph; 11 M = W, R = (CH₂)₅CH₃; 12 M = W, R = CH₂Ph) in which the ligand (Ph₂P)₂NR solely chelates the Pt atom or bridges an M–Pt bond as in [PtM₂(CO)₅Cp₂{μ-(Ph₂P)₂N(CH₂CH₂SR)-κ²P,P}] (7 M = Mo, R = (CH₂)₅CH₃; 8 M = Mo, R = CH₂Ph; 13 M = W, R = (CH₂)₅CH₃; 14 M = W, R = CH₂Ph). The synthesis of the trinuclear complexes 3, 4, 9, and 10 entails an unexpected P-phenyl bond cleavage reaction and phenyl migration onto Pt. When only 1 equiv of Na[M(CO)₃Cp] (M = Mo or W) was used, the heterodinuclear products of monosubstitution [PtCl{M(CO)₃Cp}{(Ph₂P)₂N(R)PPh₂-P,P}] (15 M = Mo, R = (CH₂)₅CH₃; 16 M = Mo, R = CH₂Ph; 17 M = W, R = (CH₂)₅CH₃; 18 M = W, R = CH₂Ph) were obtained, which are the precursors to the bicyclic products 3, 4, 9, and 10, respectively. Density functional calculations were performed to study the thermodynamics of the formation of all the new complexes, to evaluate the relative stabilities of the isomeric chelated and bridged forms, and to trace the mechanism of formation of the phosphanido-bridged products 3, 4, 9, and 10. It was concluded that Pt(II) complexes containing a thioether-functionalized short-bite ligand, [PtCl₂{(Ph₂P)₂N(R)PPh₂}], react with Na[M(CO)₃Cp] to yield first heterodinuclear Pt–M and then heterotrinuclear PtM₂ complexes resulting from the activation of a P–C bond in one of the PPh₂ groups and phenyl migration to Pt. The critical role of an intramolecular thioether group was demonstrated.



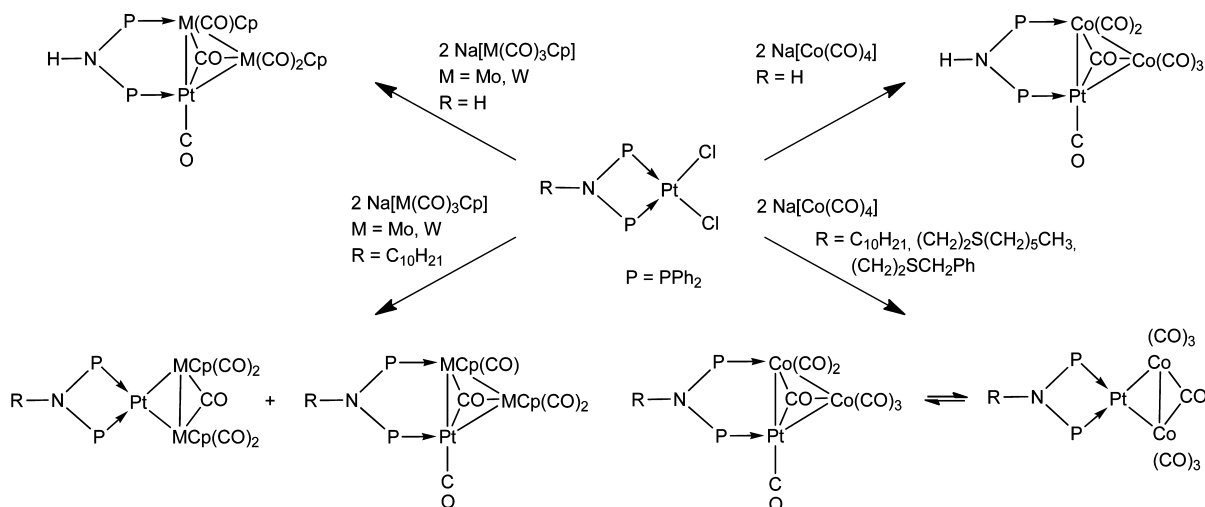
1. INTRODUCTION

Despite spectacular developments and achievements in cluster chemistry since F. A. Cotton coined the term in 1962–1963, it remains often difficult or even impossible to predict the molecular formula and structure of a cluster resulting from a chemical synthesis, even if the latter has been designed for this purpose. It is also well-recognized that reactions aiming toward the synthesis of specific cluster compounds may not be successful, while most exciting and novel structures have often resulted from serendipity. This situation results from the large

number of kinetic and thermodynamic parameters involved, their subtlety and intricacy, the diversity of metals and ligands available and, even for transition metals with similar valence shells, the differences in reactivity of the metal centers and of their ligands in the precursor molecules. In our laboratories, we have investigated the synthesis of mixed-metal trinuclear clusters with PtCo₂, PtMo₂, or PtW₂ cores, stabilized by short-bite ligands¹ such as

Received: January 29, 2015

Published: May 5, 2015

Scheme 1. Trinuclear PtCo₂, PtMo₂, or PtW₂ Clusters with dppa or N-Substituted dppa Ligands

bis(diphenylphosphanyl)methane [dppm], bis(diphenylphosphanyl)amine [dppa], and N-substituted dppa of formula $(\text{Ph}_2\text{P})_2\text{N-R}$ [$\text{R} = (\text{CH}_2)_9\text{CH}_3$, $(\text{CH}_2)_2\text{S}(\text{CH}_2)_5\text{CH}_3$, $(\text{CH}_2)_2\text{SCH}_2\text{Ph}$, Ph]. The N-functionalization was introduced to examine its stereoelectronic influence on the nature of the reaction products and the possibility to deposit/anchor the corresponding clusters on various surfaces.^{2,3} The synthetic methodology consisted in the reaction of a *P,P*-chelated, dichloro Pt(II) precursor complex with a carbonylmetalate reagent. This substitution reaction can trigger the opening of the four-membered ring M-P-C (or N-P) and afford heterometallic complexes containing a stabilizing, bridging diphosphine in a thermodynamically more favorable five-membered ring.⁴ While the use of unsubstituted dppm and dppa ligands has resulted in PtCo₂,^{5,6} PtMo₂, or PtW₂ clusters^{3,7} in which the diphosphine ligand exhibits exclusively a bridging coordination mode, that of *n*-decyl-substituted dppa $(\text{Ph}_2\text{P})_2\text{N}(\text{CH}_2)_9\text{CH}_3$ led to triangular clusters in which the diphosphine exhibits both bridging and chelating coordination modes (Scheme 1).^{3,8} It is noteworthy that the reaction of dppm with a preformed heterometallic chain complex of the type *trans*-Pt[M(CO)₃Cp]₂(NCPh)₂ resulted in the formation of the first heterobimetallic complexes containing bridging and chelating dppm ligands.⁹ The behavior of thioether-functionalized ligands $(\text{Ph}_2\text{P})_2\text{N-R}$ in which $\text{R} = (\text{CH}_2)_2\text{S}(\text{CH}_2)_5\text{CH}_3$, $(\text{CH}_2)_2\text{SCH}_2\text{Ph}$ has been reported for platinum–cobalt clusters and parallels that observed with *n*-decyl-substituted dppa, in that both bridged and chelated isomeric PtCo₂ clusters are formed.³

In the course of further studies on the reactivity of Pt(II) complexes of the type $[\text{PtCl}_2\{(\text{Ph}_2\text{P})_2\text{N}(\text{CH}_2)_2\text{SR-P,P}\}]$ ($\text{R} = (\text{CH}_2)_5\text{CH}_3$, CH_2Ph), bearing a thioether-functionalized dppa chelate, with the Mo- and W-based metalates $\text{Na}[\text{M}(\text{CO})_3\text{Cp}]$ ($\text{M} = \text{Mo}$ or W throughout the paper), we unexpectedly isolated trinuclear complexes resulting from the activation of a *P*–phenyl bond and the migration of this phenyl ring to the platinum atom. Such dramatic molecular rearrangements are relevant to cooperativity effects in heterometallic-induced reactivity.¹⁰

2. RESULTS AND DISCUSSION

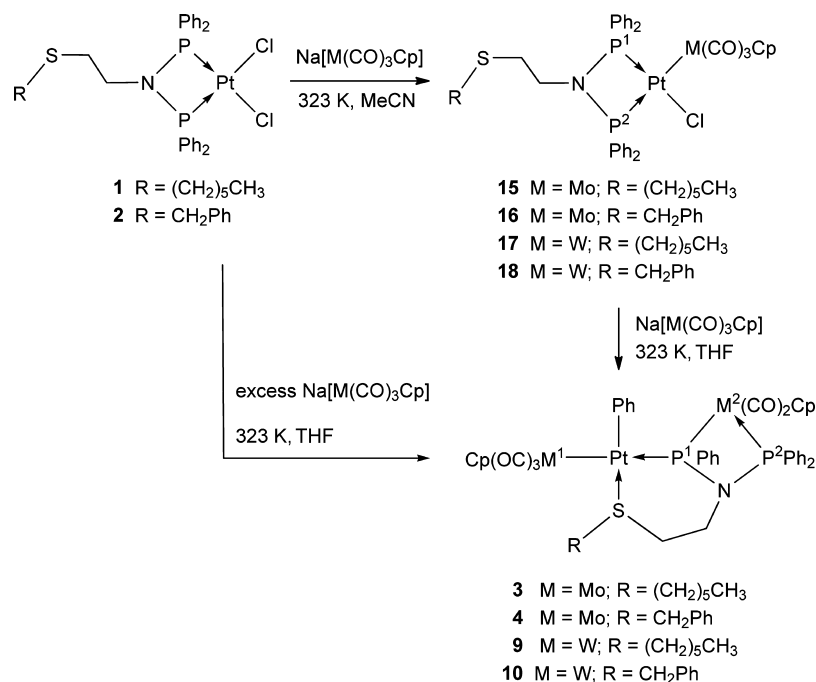
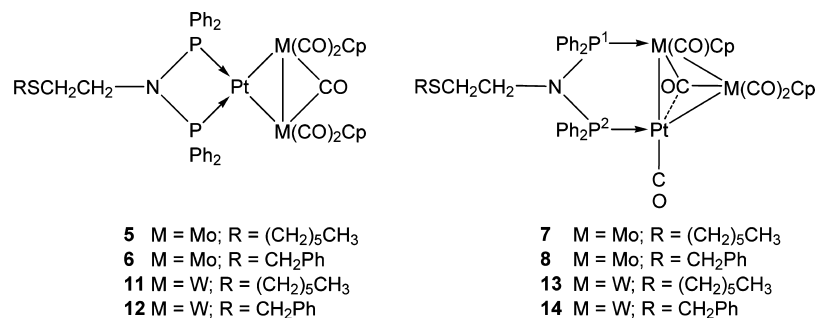
2.1. Reactivity of the Platinum Complexes 1 and 2 with $\text{Na}[\text{M}(\text{CO})_3\text{Cp}]$. The reaction of $[\text{PtCl}_2\{(\text{Ph}_2\text{P})_2\text{N}(\text{CH}_2\text{CH}_2\text{SR})-P,P\}]$ (**1** $\text{R} = (\text{CH}_2)_5\text{CH}_3$; **2** $\text{R} = \text{CH}_2\text{Ph}$) with excess $[\text{M}(\text{CO})_3\text{Cp}]^-$ at 323 K in tetrahydrofuran (THF)

led to the phosphanido-bridged trinuclear compounds $[\text{PtPh}\{\text{Mo}(\text{CO})_3\text{Cp}\}\{\mu\text{-P}(\text{Ph})\text{N}(\text{CH}_2\text{CH}_2\text{SR})(\text{PPh}_2)\text{-}\kappa^3P,P,S\}\text{Mo}(\text{CO})_2\text{Cp}]$ (**3** $\text{R} = (\text{CH}_2)_5\text{CH}_3$; **4** $\text{R} = \text{CH}_2\text{Ph}$) in 55% and 71% yield, respectively (Scheme 2). Small amounts of trinuclear clusters containing a chelating diphosphane, $[\text{PtMo}_2(\text{CO})_5\text{Cp}_2\{(\text{Ph}_2\text{P})_2\text{N}(\text{CH}_2\text{CH}_2\text{SR})\text{-}\kappa^2P,P\}]$ (**5** $\text{R} = (\text{CH}_2)_5\text{CH}_3$; **6** $\text{R} = \text{CH}_2\text{Ph}$), or a bridged diphosphane, $[\text{PtMo}_2(\text{CO})_5\text{Cp}_2\{\mu\text{-}(\text{Ph}_2\text{P})_2\text{N}(\text{CH}_2\text{CH}_2\text{SR})\text{-}\kappa^2P,P\}]$ (**7** $\text{R} = (\text{CH}_2)_5\text{CH}_3$; **8** $\text{R} = \text{CH}_2\text{Ph}$, see Table 1), were also obtained. These clusters are formula isomers; one phosphorus donor has migrated from Pt to Mo, while a CO ligand has moved from Mo to Pt.

The $^{31}\text{P}\{^1\text{H}\}$ NMR spectra of complexes **3** and **4** contain two mutually coupled doublets ($J_{P,P} = 68$ Hz for both **3** and **4**) in the region from 73 to 90 ppm. The formation of these phosphanido-bridged compounds resulted from a *P*–C bond cleavage reaction and phenyl migration from phosphorus to platinum. The thermally induced migration of a phenyl group from a coordinated phosphane ligand onto platinum has precedents in homodi- and trinuclear platinum chemistry, with the formation of, for example, the phosphanido-bridged diplatinum complex $[\text{Pt}(\text{PPh}_3)_2(\mu\text{-H})(\mu\text{-PPh}_2)\text{Pt}(\text{PPh}_3)\text{Ph}]$,^{11,12} the phosphinito complex $[\text{Pt}\{\text{PhP}(o\text{-C}_6\text{H}_4\text{CH}_2\text{O})\}(\text{Ph}_2\text{PO})(\text{Ph}_2\text{POH})\text{Ph}]$ ¹³ or the cluster $[\text{Pt}_3(\mu\text{-PPh}_2)_3\text{Ph}(\text{PPh}_3)_2]$.¹⁴

The reaction of **1** or **2** with excess $[\text{W}(\text{CO})_3\text{Cp}]^-$ at 323 K in THF similarly afforded the phosphanido-bridged complexes $[\text{PtPh}\{\text{W}(\text{CO})_3\text{Cp}\}\{\mu\text{-P}(\text{Ph})\text{N}(\text{CH}_2\text{CH}_2\text{SR})(\text{PPh}_2)\text{-}\kappa^3P,P,S\}\text{W}(\text{CO})_2\text{Cp}]$ (**9** $\text{R} = (\text{CH}_2)_5\text{CH}_3$; **10** $\text{R} = \text{CH}_2\text{Ph}$) in 34–36% yield, respectively (Scheme 2), along with the formula isomeric trinuclear clusters $[\text{PtW}_2(\text{CO})_5\text{Cp}_2\{(\text{Ph}_2\text{P})_2\text{N}(\text{CH}_2\text{CH}_2\text{SR})\text{-}\kappa^2P,P\}]$ (**11** $\text{R} = (\text{CH}_2)_5\text{CH}_3$; **12** $\text{R} = \text{CH}_2\text{Ph}$) and $[\text{PtW}_2(\text{CO})_5\text{Cp}_2\{\mu\text{-}(\text{Ph}_2\text{P})_2\text{N}(\text{CH}_2\text{CH}_2\text{SR})\text{-}\kappa^2P,P\}]$ (**13** $\text{R} = (\text{CH}_2)_5\text{CH}_3$; **14** $\text{R} = \text{CH}_2\text{Ph}$), see Table 1). The $^{31}\text{P}\{^1\text{H}\}$ NMR resonances for **9** and **10** appear as two mutually coupled doublets ($J_{P,P} = 55$ Hz for both **9** and **10**) in the region of 40–60 ppm.

When the reaction of complex **1** (or **2**) with 1 to 4 equiv of $[\text{M}(\text{CO})_3\text{Cp}]^-$ at 323 K was performed in MeCN instead of THF as solvent, it stopped at the monosubstitution products $[\text{PtCl}\{\text{M}(\text{CO})_3\text{Cp}\}\{\text{Ph}_2\text{PN}(\text{R})\text{PPh}_2\text{-}P,P\}]$ (**15** $\text{M} = \text{Mo}$, $\text{R} = (\text{CH}_2)_5\text{CH}_3$; **16** $\text{M} = \text{Mo}$, $\text{R} = \text{CH}_2\text{Ph}$; **17** $\text{M} = \text{W}$, $\text{R} = (\text{CH}_2)_5\text{CH}_3$; **18** $\text{M} = \text{W}$, $\text{R} = \text{CH}_2\text{Ph}$; Scheme 2 and Table 2). These dinuclear Pt–M complexes, likely intermediates in the synthesis of the trinuclear clusters, were detected when less than 2 equiv of $[\text{M}(\text{CO})_3\text{Cp}]^-$ was used at 323 K in THF. Their

Scheme 2. Reactivity of 1 and 2 with Na[M(CO)₃Cp]Table 1. ³¹P{¹H} NMR Data for Compounds 5–8 and 11–14 (THF, 298 K)

	R	M	δ P ¹ , ppm	δ P ² , ppm	$^2J_{P,P}$, Hz	$^1J_{P,P}$, Hz	$^1J_{P,W}$, Hz
5	(CH ₂) ₅ CH ₃	Mo	61.0			3168	
6	CH ₂ Ph	Mo	61.1			3169	
11	(CH ₂) ₅ CH ₃	W	45.5			3038	
12	CH ₂ Ph	W	47.3			3040	
7	(CH ₂) ₅ CH ₃	Mo	121.7	84.8	46	<i>a</i>	
8	CH ₂ Ph	Mo	122.1	84.6	45	<i>a</i>	
13	(CH ₂) ₅ CH ₃	W	85.2	75.8	61	4045	350
14	CH ₂ Ph	W	87.1	77.4	60	4050	349

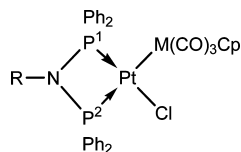
^aNot determined due to the low intensity of the signals.

³¹P{¹H} NMR data (Table 2) are very similar to those of the corresponding (Ph₂P)₂N(CH₂)₉CH₃ analogues **19** (M = Mo) and **20** (M = W).³

As already noticed for the latter complexes,³ the ³¹P{¹H} NMR signal of phosphorus P² trans to the [M(CO)₃Cp] group in **15–18** is very broad in THF at 298 K, a phenomenon that can be explained by partial dissociation of the [M(CO)₃Cp][−] moiety in THF where an equilibrium can occur between the coordinated and the (tight) ion-pair forms. The different behavior of intermediates **15–18** in acetonitrile and in THF can thus be explained by assuming that reactivity with fresh [MCp(CO)₃][−] is possible only for the ion pair present in THF.

To ascertain whether an external thioether ligand could facilitate a P–C bond activation of the type observed during the synthesis of **3**, **4**, **9**, and **10**, we performed the reaction of [PtCl₂{(Ph₂P)₂N(*n*-decyl)-*P,P'*}] with 2 equiv of Na[Mo(CO)₃Cp] in the presence of excess di-*n*-butylsulfide. The course of the reaction was identical to that performed in the absence of di-*n*-butylsulfide,¹⁵ indicating that the P–C bond activation leading to **3**, **4**, **9**, and **10**, requires the presence of a sulfur atom *within* the tail of the PNP ligand.

The structures of complexes **4** and **9** were determined by X-ray diffraction analysis. Multinuclear NMR spectroscopy indicated that the structures found in the solid state are maintained in solution. The complete analogy of spectroscopic features found

Table 2. $^{31}\text{P}\{^1\text{H}\}$ NMR Data for the Heterodinuclear Complexes 15–18 (CD_3CN , 298 K)

	R	M	δP^1 , ppm	δP^2 , ppm	$^2J_{\text{P,P}}$, Hz	$^1J_{\text{P1,P2}}$, Hz	$^1J_{\text{P2,P2}}$, Hz
15	$(\text{CH}_2)_2\text{S}(\text{CH}_2)_3\text{CH}_3$	Mo	29.2	53.8	28	3557	2648
16	$(\text{CH}_2)_2\text{SCH}_2\text{Ph}$	Mo	29.3	53.9	27	3560	2658
17	$(\text{CH}_2)_2\text{S}(\text{CH}_2)_3\text{CH}_3$	W	28.0	52.3	27	3584	2571
18	$(\text{CH}_2)_2\text{SCH}_2\text{Ph}$	W	27.5	51.7	27	3585	2574
19 ^a	$(\text{CH}_2)_9\text{CH}_3$	Mo	28.4	53.6	28	3549	2648
20 ^a	$(\text{CH}_2)_9\text{CH}_3$	W	26.6	51.6	28	3571	2583

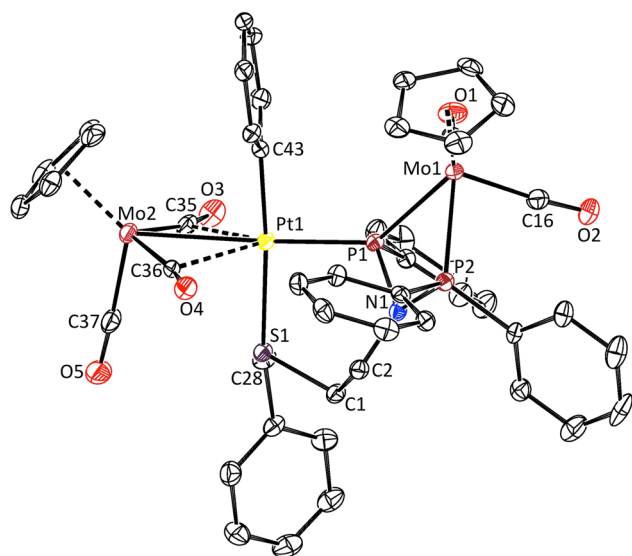
^aFrom ref 3.

Figure 1. PLATON drawing of complex **4**. Displacement ellipsoids are scaled to 30% probability, and H atoms were omitted for clarity. Selected interatomic distances (Å) and angles (deg): Pt1–C43 2.019(5), Pt1–P1 2.300(1), Pt1–S1 2.403(1), Pt1–C36 2.414(5), Pt1–C35 2.508(5), Pt1–Mo2 2.9174(5), Mo2–C35 1.964(6), Mo2–C36 1.975(5), Mo1–P2 2.452(1), Mo1–P1 2.567(1), P1–N1 1.737(4), P2–N1 1.670(4), P1–P2 2.658(2); C43–Pt1–P1 92.7(1), C43–Pt1–S1 174.5(1), P1–Pt1–S1 91.98(4), C43–Pt1–C36 91.75(17), C43–Pt1–C35 92.7(2), P1–Pt1–C36 140.4(1), P1–Pt1–C35 136.4(1), S1–Pt1–C36 82.8(1), S1–Pt1–C35 85.9(1), C35–Pt1–C36 82.6(2), C43–Pt1–Mo2 85.3(1), P1–Pt1–Mo2 176.96(3), S1–Pt1–Mo2 90.12(3), C36–Pt1–Mo2 42.2(1), C35–Pt1–Mo2 41.6(1), P2–Mo1–P1 63.91(4), C1–S1–C28 101.0(2), C28–S1–Pt1 108.7(2), C1–S1–Pt1 112.3(2), Pt1–P1–Mo1 132.88(5), C12–N1–P2 124.0(3), C12–N1–P1 125.4(3), P2–N1–P1 102.5(2), N1–P2–Mo1 99.2(1), N1–P1–Mo1 93.2(1).

for **3/4** or **9/10** allows us to assign for **3** and **10** the structures depicted in Scheme 2. The crystal structure of **4** is depicted in Figure 1.

The unusual structure of complex **4** consists of a six-membered platinumacycle condensed with a four-membered M-P-N-P cycle. The phosphanido group and the Mo-bound phosphane form a four-membered ring, while the phosphanido and the thioether groups chelate the platinum atom to give a six-membered ring. The coordination around Pt is completed with a phenyl group, which was originally attached to phosphorus, and a $[\text{Mo}(\text{CO})_3\text{Cp}]$ metalloligand. The platinum atom has a

distorted square planar coordination geometry to accommodate the steric requirements of the six-membered ring.

The Pt–Mo bond distance of 2.9174(5) Å is comparable to those reported for other complexes containing a platinum–molybdenum bond.^{9,16–20} The values of the Pt1–C35 and Pt1–C36 distances and of the O3–C35–Mo2 and O4–C36–Mo2 angles indicate a weak interaction between the Pt atom and the carbonyl ligands (Figure 1). The coordination of the thioether group to Pt results in a pyramidal geometry at sulfur with the sum of the angles $\sum\theta_s = 322.1^\circ$. The four-membered ring is almost planar since the plane defined by the atoms P1, N1, and P2 almost coincides with that defined by P1, Mo1, and P2 ($\sum\theta = 358.80^\circ$).

Complex **9** crystallizes as a THF hemisolvate, and the co-crystallized solvent molecule is disordered about a crystallographic center of inversion. The structure of the complex (Figure 2) is similar to that of **4** from which it differs by the nature of the S-substituent (*n*-hexyl instead of benzyl) and of the group 6 metal (W replacing Mo).

The Pt–W bond distance of 2.9158(4) Å in **9** is comparable to those reported for other complexes containing a platinum–tungsten bond.^{16,21–28} In this case too, there is a weak interaction between the Pt and the W2-bound carbonyl ligands, as indicated by the values of the Pt1–C34 and Pt1–C35 distances and of the O5–C34–W2 and O3–C35–W2 angles. The sum of the angles at the pyramidal sulfur is $\sum\theta_s = 320.1(3)^\circ$. The four-membered ring P1, N1, P2, and W1 is almost planar, with a maximum displacement of 0.012(5) Å for N1.

The percentage of pyramidal character (P.P.C.) at nitrogen, calculated according to Farrar²⁹ by the sum $\sum\theta_N$ of the angles at nitrogen, can be used to compare the strain of the four-membered P1–N1–P2–M¹ ring in **4** and **9**. With $\sum\theta_N$ values of 351.9(4) for **4** and 356.6(4) for **9**, the corresponding P.P.C. of 25.7% and 10.8%, respectively, indicate that the P1–N1–P2–Mo ring is more strained than the corresponding P1–N1–P2–W ring.

In the $^{31}\text{P}\{^1\text{H}\}$ NMR spectra of **9** (Figure 3) and **10**, the bridging P¹ atoms gives rise to doublets at δ 59.0 (60.0) flanked by ^{195}Pt and ^{183}W satellites from which the coupling constants $^1J_{\text{P,Pt}} = 2904$ (2875) Hz and $^1J_{\text{P,W}} = 158$ (156) Hz, respectively, could be extracted. The tungsten-bound P² gives rise to a doublet at δ 39.9 (41.5) flanked by ^{195}Pt and ^{183}W satellites ($^2J_{\text{P,Pt}} = 23$ (20) Hz, $^1J_{\text{P,W}} = 231$ (230) Hz). For the corresponding Mo complexes **3** and **4**, the ^{31}P signals are downfield-shifted with respect to the W analogues, the phosphanido nucleus P¹ resonates at δ 88.7 ($^1J_{\text{P,Pt}} = 2849$ Hz in **3**, $^1J_{\text{P,Pt}} = 2819$ Hz in **4**),

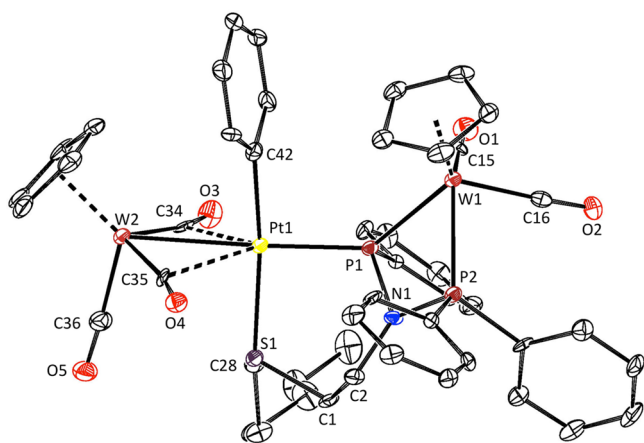


Figure 2. PLATON drawing of complex **9** in 9·0.5THF. Displacement ellipsoids are scaled to 50% probability; the solvent molecule and H atoms were omitted for clarity. Selected interatomic distances (Å) and angles (deg): Pt1–P1 2.300(2), Pt1–S1 2.415(2), Pt1–W2 2.9157(4), Pt1–C42 2.032(6), Pt1–C34 2.518(6), Pt1–C35 2.392(6), W2–C34 1.964(7), W2–C35 1.959(6), W2–C36 1.942(7), W1–P1 2.548(2), W1–P2 2.462(2), W1–C15 1.968(7), W1–C16 1.962(7); P1–Pt1–S1 92.22(5); C42–Pt1–P1 93.8(2); C42–Pt1–W2 85.3(2); S1–Pt1–W2 88.99(4); O3–C34–W2 166.1(5); O4–C35–W2 167.6(5); Pt1–S1–C1 112.6(2); Pt1–S1–C28 107.5(2); C1–S1–C28 100.0(3); C2–N1–P1 126.1(4); C2–N1–P2 126.5(4); P1–N1–P2 104.0(3); N1–P1–W1 93.00(2); N1–P2–W1 98.6(2); P1–W1–P2 64.45(5).

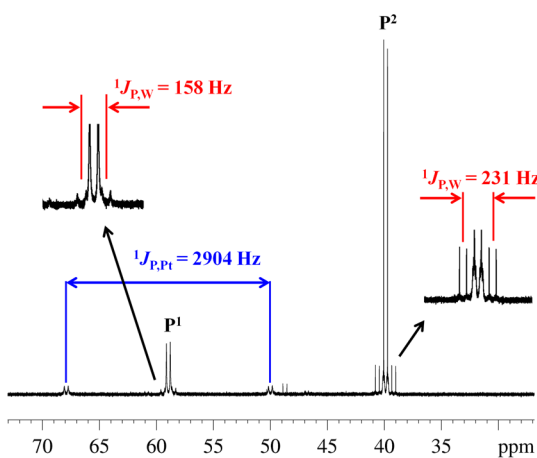


Figure 3. $^{31}\text{P}\{^1\text{H}\}$ NMR spectrum of **9** (THF- d_8 , 298 K).

and the phosphane nucleus P^2 resonates at δ 73.1 in **3** and at 73.2 in **4**. In all cases, the $^{31}\text{P}\{^1\text{H}\}$ NMR spectra showed broad P^1 signals ($\Delta\nu_{1/2}$ ranging from 5 to 12 Hz) and relatively sharp P^2 signals ($\Delta\nu_{1/2} = 2$ Hz), consistent with the existence, in THF solution, of ion pairs of formula $[\text{M}(\text{CO})_3\text{Cp}][\text{PtPh}\{\mu\text{P}(\text{Ph})\text{N}(\text{CH}_2\text{CH}_2\text{SR})(\text{PPh}_2)\text{-}\kappa^3\text{P,P,S}\}\text{M}(\text{CO})_2\text{Cp}]^+$ ($\text{M} = \text{Mo}$ or W ; $\text{R} = (\text{CH}_2)_5\text{CH}_3$ or CH_2Ph).

The ^{195}Pt NMR signal for the PtMo_2 complexes is found at δ -3508 (**3**) and δ -3517 (**4**) and for the PtW_2 complexes at δ -3591 (**9**) and δ -3605 (**10**). A detailed NMR study was performed for the structurally characterized PtW_2 complex **9**.

The ^1H NMR spectrum of **9** consists of three regions characteristic for the aliphatic protons (3.6–0.5 ppm), the cyclopentadienyl protons (5.1–4.5 ppm), and the phenyl protons (8.5–6.5 ppm). In the aliphatic region, the most deshielded signals were assigned to the $-\text{NCH}_2$ (δ 3.22 and 3.01), $-\text{CH}_2\text{SCH}_2\text{CH}_2\text{N}$ (δ 2.73 and 2.24), and $-\text{CH}_2\text{SCH}_2\text{CH}_2\text{N}$

(δ 2.36) protons by combining the information obtained from $^1\text{H}-^{195}\text{Pt}$ HMQC and ^1H COSY experiments at 298 K, whereas the remaining signals (11 H) were ascribed to the C_3H_{11} ligand tail. The cyclopentadienyl protons gave rise to two singlets at δ 4.92 and δ 4.75, which were assigned on the basis of a $^1\text{H}-^{31}\text{P}$ HMQC experiment at 298 K. The signal at δ 4.92 is scalar-coupled to both P atoms and ascribed to the Cp bonded to W^1 , while the signal at δ 4.75 showed no correlation to P and was attributed to the Cp bonded to W^2 (Chart 1). The $^1\text{H}-^{31}\text{P}$

Chart 1

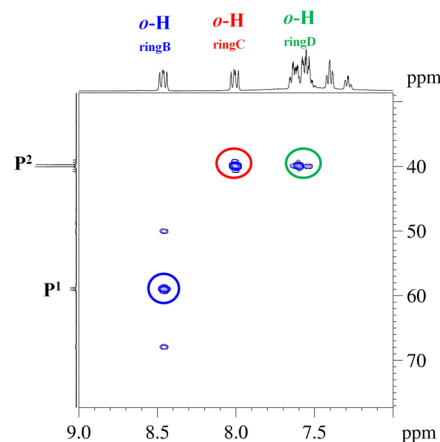
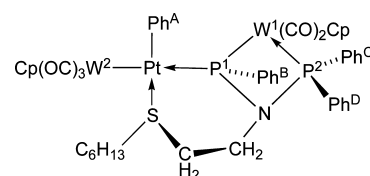


Figure 4. $^1\text{H}-^{31}\text{P}$ HMQC spectrum of **9** (phenyl region, 298 K, THF- d_8).

HMQC spectrum at 298 K (Figure 4) showed, in the phenyl region, intense cross peaks between the ortho protons of Ph^B (δ 8.41), Ph^C (δ 7.96), and Ph^D (δ 7.55) rings (Chart 1) and the P atoms to which these rings are bonded. The ortho protons of Ph^A were found at δ 7.41, in a spectral region crowded by overlapping signals, by means of a $^1\text{H}-^{195}\text{Pt}$ HMQC experiment performed at 330 K in THF- d_8 (Figure 5).

Once the ortho protons of the Pt-bound phenyl ring A were identified, the corresponding meta (δ 6.77) and para (δ 6.62) protons of this ring were easily assigned by ^1H COSY at 330 K. The fact that the $^1\text{H}-^{195}\text{Pt}$ correlation between the ortho protons of the phenyl ring A and Pt was not apparent in the $^1\text{H}-^{195}\text{Pt}$ HMQC spectrum recorded at 298 K must be ascribed to the very broad signals for the ortho protons of the phenyl ring A at 298 K, presumably due to hindered rotation of the phenyl ring about the $\text{C}_{\text{ipso}}-\text{Pt}$ bond. On raising the temperature to 330 K, the phenyl rotation is facilitated, and the very broad signal at 298 K for the meta protons of phenyl ring A becomes a sharper, pseudotriplet at 330 K.

The C_{ipso} signals of the four phenyl rings, attributed by means of $^{13}\text{C}\{^1\text{H}\}$ APT and $^1\text{H}-^{13}\text{C}$ HMBC experiments at 298 K, were found at δ 142.4 ($J_{\text{C,P}} = 7$ Hz) for ring A, δ 143.7 ($J_{\text{C,P}} = 9$ Hz) for ring B, and δ 138.7 ($J_{\text{C,P}} = 43$ Hz) and δ 133.5 ($J_{\text{C,P}} = 50$ Hz) for rings C and D, respectively. The para-C atom of ring A gave a

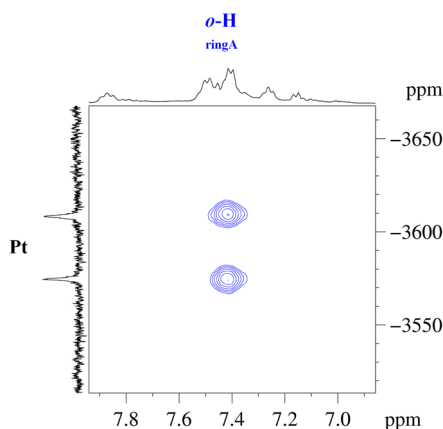


Figure 5. ^1H - ^{195}Pt HMQC spectrum of **9** (phenyl region, 330 K, THF- d_6).

singlet at δ 122.7 at 298 K, while the corresponding ortho- and meta-C signals were not detected at 298 K.

The main spectroscopic features of complexes **3**, **4**, and **10** were similarly extracted and are reported in the Experimental Section. For the PtMo₂ complex **3**, the ortho protons of phenyl ring A (bonded to Pt) appear in the ^1H NMR spectrum recorded in C₆D₆ at 298 K as a doublet centered at δ 7.91, as undoubtedly indicated by the combination of the ^1H - ^{31}P HMQC and ^1H COSY experiments, which is flanked by ^{195}Pt satellites ($^3J_{\text{H,Pt}} = 50$ Hz). The corresponding resonance for the meta protons (at δ 6.87) is quite sharp, indicating that, if present, hindered rotation

about the C_{ipso}-Pt bond is less important than for the PtW₂ analogue **9**. The IR spectra of complexes **3**, **4**, **9**, and **10** in THF showed three bands between 1786 and 1976 cm⁻¹ (see Experimental Section) for the terminal carbonyls bonded to Mo or W.

The high-resolution mass spectrometry (HRMS(+)) spectrograms of complexes **3**, **4**, **9**, and **10** recorded with a collision energy of 10 eV, applied at the exit of the quadrupole,³⁰ showed in all cases intense peaks resulting from loss of [M(CO)₃Cp]⁻. On lowering the collision energy to 2.0 eV, complex **3** led also to the peaks attributable to the [M + H]⁺ cation, while complexes **4** and **10** led to the peaks attributable to the [M]⁺ cation, and complex **9** led to the peak for [M + Na]⁺. Figure 6 shows the comparison between the experimental signals and the isotope pattern calculated for [3+H]⁺ on the basis of the natural abundances.

2.2. Reactivity with Halide Ions. Complexes **3**, **4**, **9**, and **10** are stable in the solid state and in THF or aromatic solvents but promptly react with halide ions to give the substitution products **21**–**26** (Scheme 3 and Table 3) in which the Pt-bound metalate [M(CO)₃Cp]⁻ is replaced by the incoming halide. All reactions depicted in Scheme 3 were quantitative, as ascertained by solution NMR spectroscopy.

The reactions of **3**, **4**, **9**, and **10** with solid [*n*-Bu₄N]Cl in THF afforded quantitatively the corresponding yellow chlorido complexes **21**–**24**, while reactions of **4** with [*n*-Bu₄N]Br or [*n*-Bu₄N]I yielded the yellow bromido and iodido complexes **25** and **26**, respectively (Scheme 3). To overcome the difficulty of

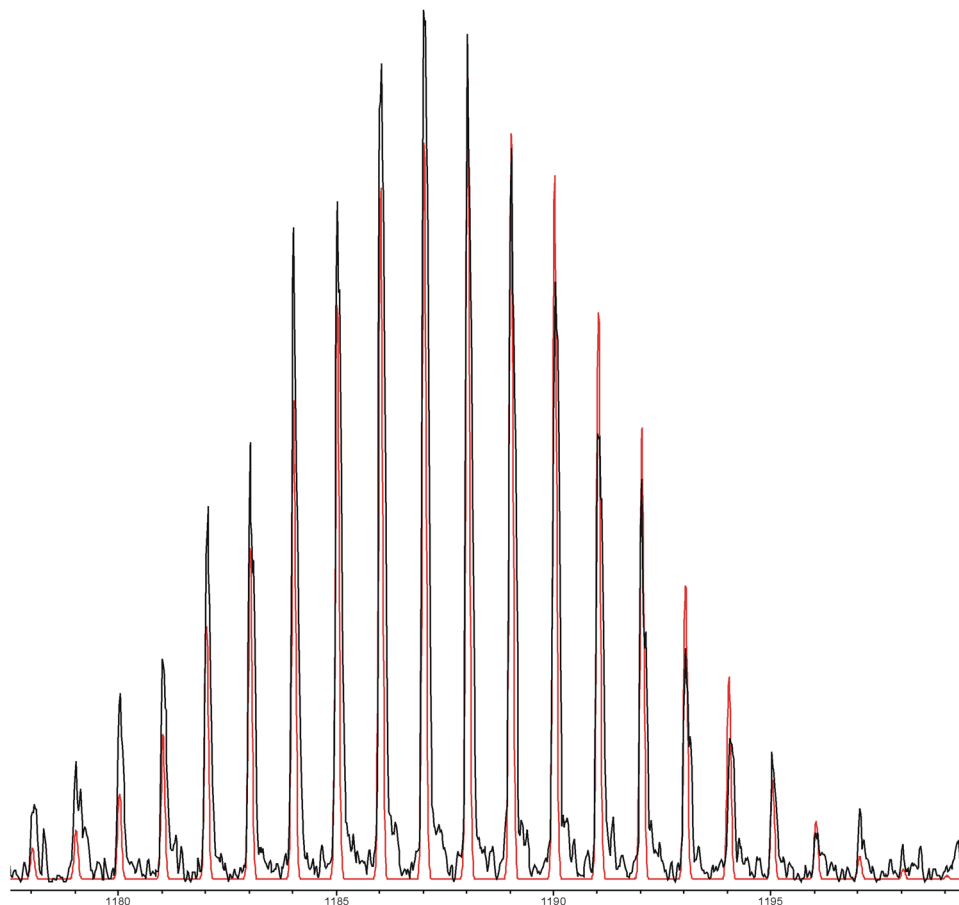
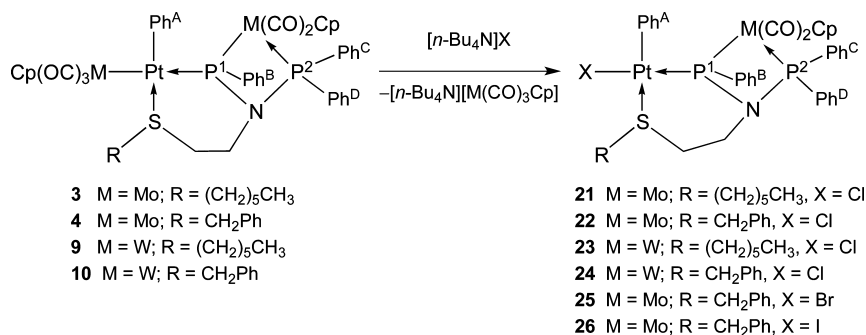


Figure 6. Experimental (black) and calculated (red) HRMS(+) spectrogram of the [M + H]⁺ ion of **3** (exact mass = 1188.0492 da,³¹ measured 1188.0368) in acetone. The error between calculated and observed isotope patterns is 0.5 ppm.

Scheme 3. Reactivity of Complexes 3, 4, 9, 10 with Halides

Table 3. ³¹P{¹H} NMR Data for the Halido-Complexes 21–29 (THF, 298 K)

compound	R	M	X	Y	δ P ¹ , ppm	δ P ² , ppm	² J _{P,P} , Hz	¹ J _{P,Pt} , Hz
21	(CH ₂) ₅ CH ₃	Mo	Cl	Ph ^A	72.8	71.9	74	3582
22	CH ₂ Ph	Mo	Cl	Ph ^A	75.0	74.6	75	3576
23 ^a	(CH ₂) ₅ CH ₃	W	Cl	Ph ^A	43.8	43.2	62	3713
24	CH ₂ Ph	W	Cl	Ph ^A	45.2	42.8	62	3634
25	CH ₂ Ph	Mo	Br	Ph ^A	75.5	74.7	74	3541
26	CH ₂ Ph	Mo	I	Ph ^A	73.6	74.9	71	3393
27	CH ₂ Ph	Mo	I	I	65.1	77.8	74	2653
29	CH ₂ Ph	Mo	Cl	Cl	62.0	80.4	85	2969

^ain CDCl₃.

removing the anion [Mo(CO)₃Cp][−] liberated in the reaction, we performed the reaction between **4** and [n-Bu₄N]X in THF under O₂ bubbling. Under these conditions, [Mo(CO)₃Cp][−] is readily oxidized in oxo species,^{9,32} which were easily separated from the reaction mixture.

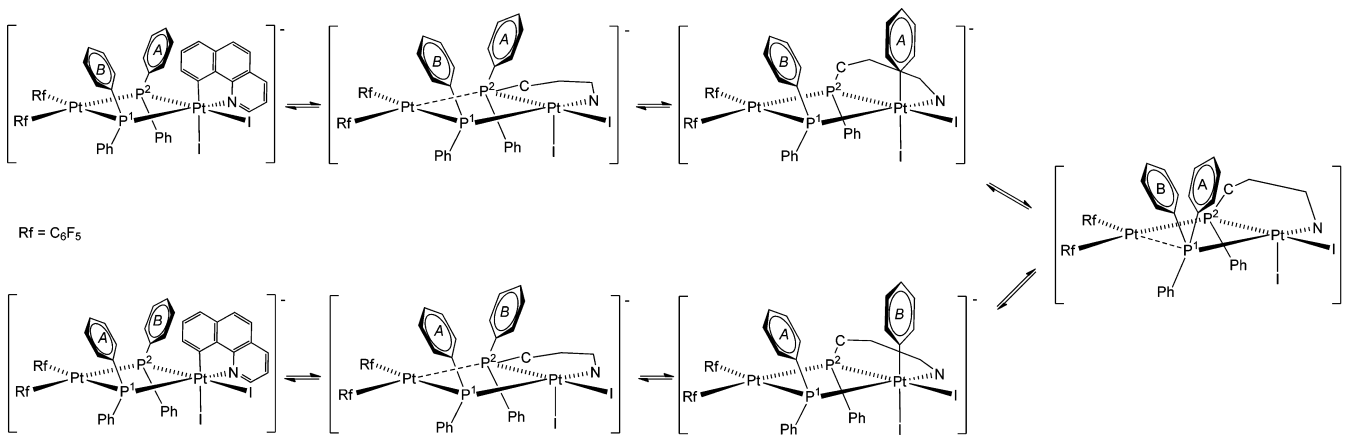
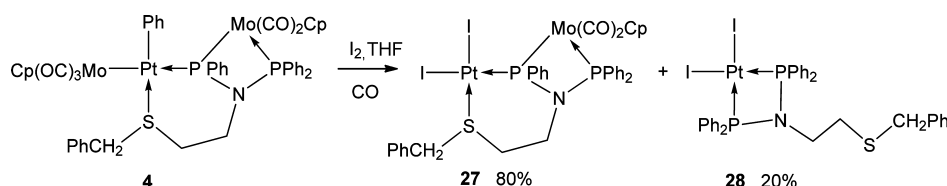
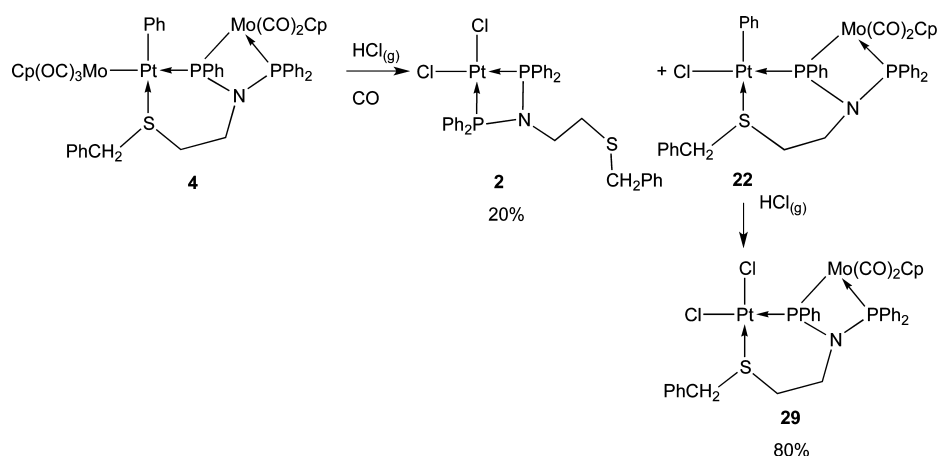
Some lability of the Pt-bound [M(CO)₃Cp] group in **3**, **4**, **9**, and **10** may be anticipated from the ion pair structure present in solutions as suggested by ³¹P NMR. Furthermore, the easy loss of [M(CO)₃Cp][−] during the electrospray ionization mass spectrometry(+) analysis of **3**, **4**, **9**, and **10** is consistent with the lability of this group. The ease of replacement of [M(CO)₃Cp][−] with a halide explains why a quantitative transformation into **21–24** was observed when the trinuclear complexes **3**, **4**, **9**, and **10** were percolated through a silica chromatographic column using CHCl₃ as eluent.

The HRMS(+) spectrogram of **22**, **25**, and **26** recorded in MeOH/HCOOH showed the peaks due to [M–X]⁺ (X = Cl, Br, or I) and those attributable to [M+K]⁺ (1022.9945 Da for **22**, 1050.9716 Da for **25**, and 1098.9589 Da for **26**). The solid-state IR spectra of **22**, **25**, and **26** were almost superimposable, showing two very strong carbonyl stretching bands around 1966 and 1893 cm^{−1}. The ν(Pt–Cl) IR absorption band of the chlorido complex **22** was observed at 280 cm^{−1}. The structure of complexes **21**, **23**, and **24** was inferred from their spectroscopic features by comparison with those of **22**. For **21–26**, the P² NMR signal remained nearly unchanged, while that of P¹ was upfield-shifted by 15–20 ppm. As expected from the different trans influences of M(CO)₃Cp and X (X = Cl, Br, I), the direct ³¹P–¹⁹⁵Pt coupling constants of P¹ increases by ca. 600 Hz on going from **3**, **4**, **9**, and **10** to **21–26**. The ¹⁹⁵Pt NMR signal is

shifted to higher fields on going from **22** (Cl, δ –4034), **25** (Br, δ –4110) to **26** (I, δ –4297). The coordination to Pt of the phenyl group Ph^A and of the thioether S atom was confirmed by ¹H–¹⁹⁵Pt HMQC experiments, which showed the correlations between the ¹⁹⁵Pt and both the ortho protons of Ph^A and the two methylene protons bonded to S.

2.3. Reverse Migration of the Phenyl Group. Metal-mediated P–C bond cleavage reactions are well-documented (especially for PPh₃ and dppm) and are not only relevant to possible catalyst deactivation mechanisms³³ but often give rise to new stable organometallic species resulting from molecular rearrangements.^{34–43} However, only few systems have been reported in which the original P–C bond can be reformed. The first example of this kind was reported in 1976 and deals with the reversible oxidative addition of PPh₃ to zerovalent nickel and palladium complexes.⁴⁴ Subsequently, the reversible phenyl migration between iron and phosphorus on a phosphoranide complex,⁴⁵ the reversible thermal phenyl migration from PPh₃ on a triruthenium carbonyl cluster,⁴⁶ and the reversible phenyl migration from Ru to P in a BINAP complex, without loss of stereogenicity at the metal atom,⁴⁷ have been described. As far as platinum chemistry is concerned, a ¹H EXSY analysis has demonstrated the exchange between rings A and B in the dinuclear diphenylphosphanido-bridged benzoquinoline complex [NBu₄][(R^F)₂Pt(μ-PPh₂)₂Pt(C₁₃H₈N-κ²N,C)] (R^F = C₆F₅; C₁₃H₈N = benzoquinoline), as a result from a reversible P–C bond breaking reaction (Scheme 4).⁴⁸

In the same study, it was shown that treating [NBu₄][(R^F)₂Pt(μ-PPh₂)₂Pt(C₁₃H₈N-κ²N,C)] (R^F = C₆F₅; C₁₃H₈N = benzoquinoline) with I₂ resulted in P–C bond formation between a bridging PPh₂ and the coordinated benzoquinoline. This type of

Scheme 4. Reversible P–C Bond Breaking Occurring in a Dinuclear Diphenylphosphanido-Bridged Benzoquinolate Pt Complex⁴⁸Scheme 5. Reactivity of **4** with Iodine and Migration of the Phenyl Group from Pt to PScheme 6. Reactivity of **4** with HCl

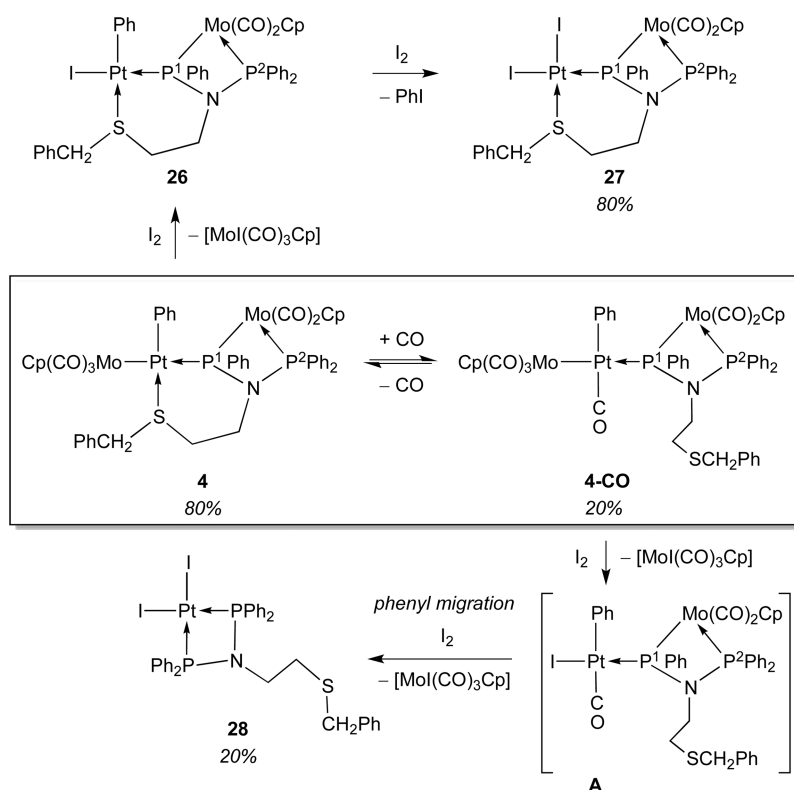
I₂-induced P–C bond formation was not unprecedented: it has been reported for the cluster [Pt₃(μ-PPh₂)₃Ph(PPh₃)₂] when its Pt-bound phenyl group migrates to phosphorus to give [Pt₃(μ-PPh₂)₃(μ-I)(PPh₃)₃]⁴⁹ and for several polynuclear diphenylphosphanido-bridged platinum and palladium complexes bearing pentafluorophenyl groups, which give coordinated PPh₂(C₆F₅) as the result of reductive coupling.^{50–52}

To test whether molecular iodine could induce phenyl migration from platinum back to P¹ in our trinuclear species, we treated **4** with I₂ in THF under 1 atm of CO at room temperature for 4 h. The reaction led to a mixture of [PtI₂{μ-P(Ph)-N(CH₂)₂SCH₂Ph}(PPh₂)-κ³P,P,S}M(CO)₂Cp] (**27**) (80%) and *cis*-[PtI₂{(Ph₂P)₂N(CH₂)₂SCH₂Ph-P,P}] (**28**, 20%, Scheme 5). The formation of **28** requires that phenyl migration has occurred from platinum to phosphorus, and this demonstrates that in our system, P–C and Pt–C bond activation can be thermally and chemically triggered, respectively. Depending on the conditions, phenyl migration can thus occur from P to Pt or from Pt to P.

The structure of the reaction products **27** and **28** was confirmed by comparison of their spectroscopic features with those

of authentic samples: **27** was prepared by reaction of **26** with I₂ and **28** by reaction of [PtI₂(cod)] with the ligand (Ph₂P)₂N(CH₂)₂SCH₂Ph. Monitoring of the reaction of Scheme 5 by ³¹P NMR revealed that after 20 min the starting material **4** was consumed and that the THF solution contained 20% of **28** and 80% of **26**. After 1 h of reaction, the amount of **28** was unchanged (20%), but **26** progressively transformed into **27**, giving a solution containing 32% of **26** and 48% of **27**. After 4 h, the continuing transformation of **26** into **27** afforded a solution containing only **27** (80%) and **28** (20%). These data indicate that **4** reacts with 2 equiv of iodine to give first **26** and **28**, complex **27** resulting from further iodination of **26**. That **26** is the precursor to **27** and not to **28** was confirmed by the reaction of **26** with an equimolar amount of I₂ in THF at 298 K, which afforded quantitatively **27** and PhI,⁵³ without any formation of **28**.⁵⁴

The synthesis of **28** entails the loss of the Mo^I(CO)₂Cp fragment as [MoI(CO)₃Cp], which was actually detected by IR spectroscopy (diagnostic band at 2040 cm⁻¹)^{55,56} as the only mononuclear molybdenum carbonyl species present in solution after the reaction mixture was stirred for 4 h. The formation of

Scheme 7. Proposed Steps in the Reaction of **4** with I_2 under CO Atmosphere

this complex requires the presence of external CO. To examine the effect of CO on the selectivity of the reaction between **4** and I_2 in THF at 298 K, an experiment was performed in the absence of external CO. This afforded, after 1 h of reaction, complex **26** in >95% spectroscopic yield and only traces (<5%) of **28**,⁵⁷ indicating a beneficial effect of CO for directing the iodination of **4** toward the product of phenyl transfer **28**.

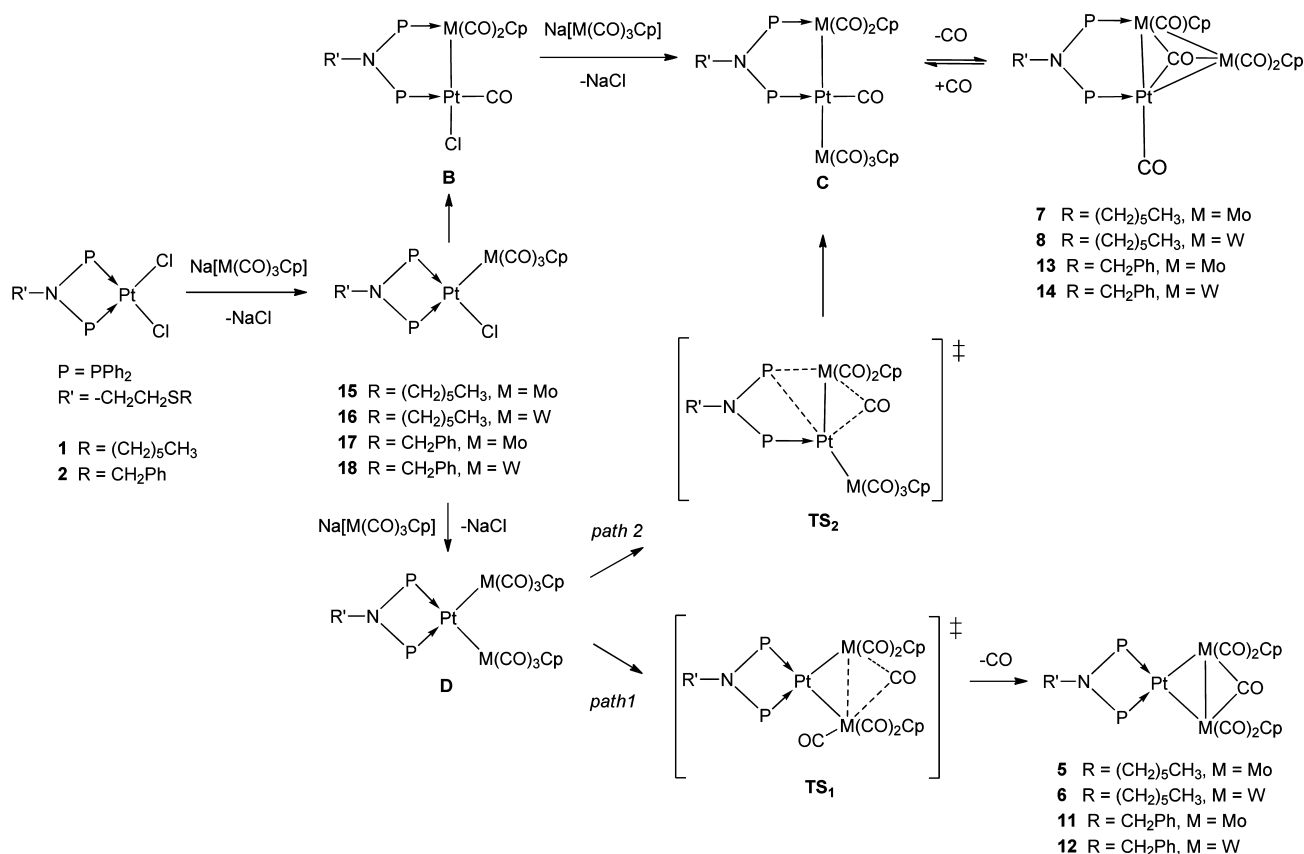
The phenyl transfer back from Pt to P^1 was also observed when **4** was reacted with gaseous HCl. The reaction, performed in THF under 1 atm of CO led, after 20 h, to a mixture containing 20% of **2**, the product of phenyl migration from platinum to phosphorus, analogous to **28**, and ca. 80% of **29** (Scheme 6). When performed in the absence of external CO, the same reaction led quantitatively to **29**, with formation of benzene (gas chromatography-mass spectrometry). Monitoring the reaction between **4** and HCl/CO revealed that **2** forms at an early stage of the reaction, and as soon as **4** is consumed (less than 20 min), the amount of **2** in solution remains steady, while the monochlorido species **22** is converted into **29** by the excess of HCl. The intermediacy of **22** also shows that the Mo–Pt bond in **4** is more reactive toward $HCl(g)$ than the more covalent Pt–Ph bond.

The identical yield of the phenyl migration product (20%) and the nonphenyl-migrated product (80%) for both the I_2 /CO (Scheme 5) and the HCl/CO reactions (Scheme 6) suggests a common mechanism, in which the presence of CO plays a crucial role. Thus, it is conceivable that **4** could give rise to the equilibrium depicted in Scheme 7 where CO reversibly coordinates to the Pt center of the ion pair, displacing the sulfur atom. The outcome of the reactions with I_2 (or HCl) can be rationalized by assuming that the carbonylated product **4-CO** is present in the equilibrium mixture in a ca. 20% amount and that complex **4-CO** is the precursor to the migration products **28** (or **2**), while the remaining 80% of **4** is the precursor to the dinuclear species **26** and **27** (or **22** and **29**). The pathways proposed for the reaction

of **4** with I_2 or HCl are depicted in Scheme 7 and in Supporting Information, Scheme S1, respectively.

To substantiate the mechanism proposed for explaining the similar reactivity exhibited by **4** with I_2 or HCl, we investigated the reaction of CO alone with complex **4**. Placing a THF solution of **4** under CO at 298 K caused the formation of a new species, whose spectroscopic features are compatible with the formula proposed for **4-CO**. The $^{31}P\{^1H\}$ spectrum of the solution showed, beside signals ascribed to **4**, two mutually coupled doublets ($^2J_{P,P} = 67$ Hz) at δ 81.6 and δ 118.7, the latter flanked by ^{195}Pt satellites ($^1J_{P,Pt} = 2403$ Hz), in a **4-CO**/**4** integral ratio of 20:80, and ascribable to P^2 and P^1 of **4-CO**, respectively (see Scheme 7 for numbering). Moreover, by performing the carbonylation of **4** with ^{13}CO , it was possible to detect the ^{13}C NMR signal of the Pt-bound carbonyl of **4-CO** as a doublet ($^2J_{C,P} = 3$ Hz) at δ 183.9 flanked by ^{195}Pt satellites ($^1J_{C,Pt} = 1014$ Hz). The appearance of the signal at δ 118.7 as a doublet (and not as a doublet of doublets) also when ^{13}CO was used, along with the small value for the geminal ^{13}C – ^{31}P coupling constant (3 Hz, not resolved in the ^{31}P NMR spectrum owing to the broadness of the P^1 signal) indicates that the carbonyl ligand replaces the sulfur atom rather than the $Mo(CO)_3Cp$ anion, thus substantiating the formula proposed for **4-CO**.

According to Scheme 7, the carbonylated species **4-CO** could react with iodine to give intermediate **A**, which, in turn, can give **28** by loss of the $Mo^1(CO)_2Cp$ fragment (in the form of $[MoI(CO)_3Cp]$), phenyl transfer back to P^1 , and coordination of P^2 and of an external iodide (not necessarily in this sequence). Although the collected data are insufficient to determine with certainty the reaction profile for the transformation from **4-CO** to **28**, we propose that the phenyl transfer occurs after loss of the $Mo^1(CO)_2Cp$ fragment that leaves the Pt-bound P^1 atom with a phosphonium character favorable to accept aryl migration.^{58,59}

Scheme 8. Proposed Mechanism for the Formation of the Bridged and Chelated Trinuclear PtM₂ Clusters

2.4. Density Functional Theory Studies. Density functional theory (DFT) calculations at the M06/LACV3P+**//M06/LACVP* level were performed to study the thermodynamics of the transformations and trace a possible mechanism for the formation of the condensed six-membered platinacycle and four-membered M'-P-N-P-cycle complexes 3-4 and 9-10, explaining the role of the sulfur on the N-substituted dppa ligand.

In a recent DFT study on the reactivity of mononuclear Pt complexes analogous to 1 and 2, but containing a *n*-decyl-substituted dppa, with Na[M(CO)₃Cp], which led only to the formation of dinuclear PtM (analogous to 15-18) and trinuclear PtM₂ (analogous to 5-8 and 11-14) complexes, we found geometries and relative stabilities of the chelated and bridged isomers of the PtM₂ clusters in good agreement with all the experimental data available, thus showing that the M06/LACV3P+**//M06/LACVP* level of theory employed was sufficiently adequate to deal with this class of trinuclear complexes.³

The reliability of this level of theory in reproducing also the geometrical parameters of the new six-membered platinacycle complexes was confirmed by a geometry optimization of the structurally characterized complexes 4 and 9, which gave bond lengths and angles within 0.06 Å and 4°, respectively, of the experimental data.

On the basis of experimental data and DFT calculations, we also proposed a reaction mechanism for the formation of the dinuclear PtM and the triangular PtM₂ species, the only products isolated when an *n*-decyl-substituted dppa ligand was employed.³ An analogous mechanism, see Scheme 8, is suggested for the reaction of 1,2 with Na[M(CO)₃Cp], which leads to the

monosubstitution products 15-18 and to the chelated 5,6 and 11,12 and bridged 7,8 and 13,14 trinuclear clusters, while the formation of the final complexes 3,4 and 9,10 allegedly occurs from one of the intermediates in this mechanism through the intervention of the sulfur atom of the thioether dppa substituent. Accordingly, the first step would consist of the nucleophilic substitution of the [M(CO)₃Cp]⁻ anion for a Cl⁻ ligand of 1 or 2, leading to the corresponding monosubstitution dinuclear products 15-18: two possible isomers can be formed for each of these dinuclear species, 15-18 and B, corresponding to the chelate or bridged coordination of the diphosphanylamine. These monosubstituted complexes undergo a second nucleophilic substitution step whereby the remaining chloride ligand on Pt is replaced by the second [M(CO)₃Cp]⁻ anion. The second substitution on the bridged isomer B is expected to lead to a trinuclear chain complex C, observed only for R = H,⁵ which then loses a carbonyl group and forms a M-M bond to give the bridged clusters 7,8 or 13,14. The second substitution on the chelate isomer 15 is instead expected to lead to a trinuclear PtM₂ species D whose evolution may follow two different pathways: (i) formation of a M-M bond between the two cis M(CO)₃Cp groups with loss of a carbonyl ligand and migration of a carbonyl to a bridging position, resulting in the chelate clusters: 5,6 or 11,12 (path 1); (ii) shift of one of the phosphorus atoms from Pt to the adjacent M atom with simultaneous migration of a CO from the P-bonded M to the Pt center—that is, change in the coordination of the N-substituted dppa from chelated to bridged—leading to the linear chain complexes C, which would then evolve to the bridged clusters 7,8 or 13,14 (path 2).

We first calculated the thermodynamics of the formation of the monosubstitution products 15-18, the chelated triangular

Table 4. Relative Enthalpies and Free Energies in THF^a

	15–18	B	D	C	7,8 and 13,14	5,6 and 11,12	3,4 and 9,10
Enthalpy							
M = Mo, R = (CH ₂) ₅ CH ₃	-35.7	-28.7	-66.7	-73.2	-49.3	-55.5	-61.3
M = Mo, R = CH ₂ Ph	-40.1	-33.4	-70.0	-72.6	-50.0	-54.9	-63.2
M = W, R = (CH ₂) ₅ CH ₃	-36.1	-27.9	-54.2	-70.1	-45.1	-54.2	-62.0
M = W, R = CH ₂ Ph	-38.1	-31.5	-69.8	-72.8	-46.7	-54.1	-63.7
Free Energy							
M = Mo, R = (CH ₂) ₅ CH ₃	-23.6	-14.6	-38.3	-41.9	-30.9	-40.0	-43.5
M = Mo, R = CH ₂ Ph	-28.0	-19.1	-44.3	-47.4	-34.1	-39.9	-49.7
M = W, R = (CH ₂) ₅ CH ₃	-24.0	-15.2	-34.0	-41.1	-26.2	-34.0	-43.7
M = W, R = CH ₂ Ph	-25.5	-17.0	-43.6	-45.4	-30.9	39.0	-50.1

^aThe tabulated values correspond to the formation of the dinuclear PtM species 15–18, the triangular PtM₂ clusters 7,8, 13,14 (chelated) and 5,6, 11,12 (bridged), the intermediates B–D, and to the six-membered platinacycle complexes 3, 4, 9, and 10 obtained from the mononuclear Pt complexes 1, 2, and 1 or 2 equiv of Na[M(CO)₃Cp], according to the mechanism reported in Scheme 6.

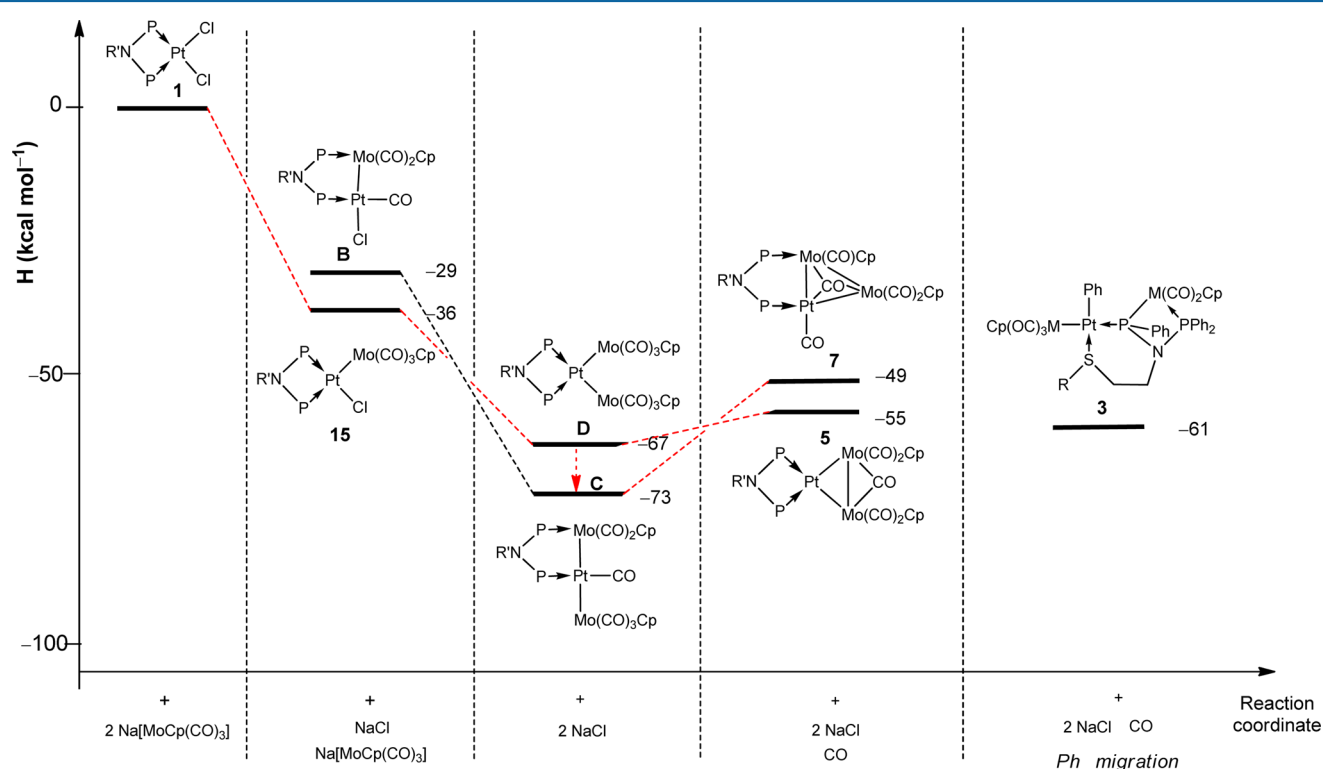


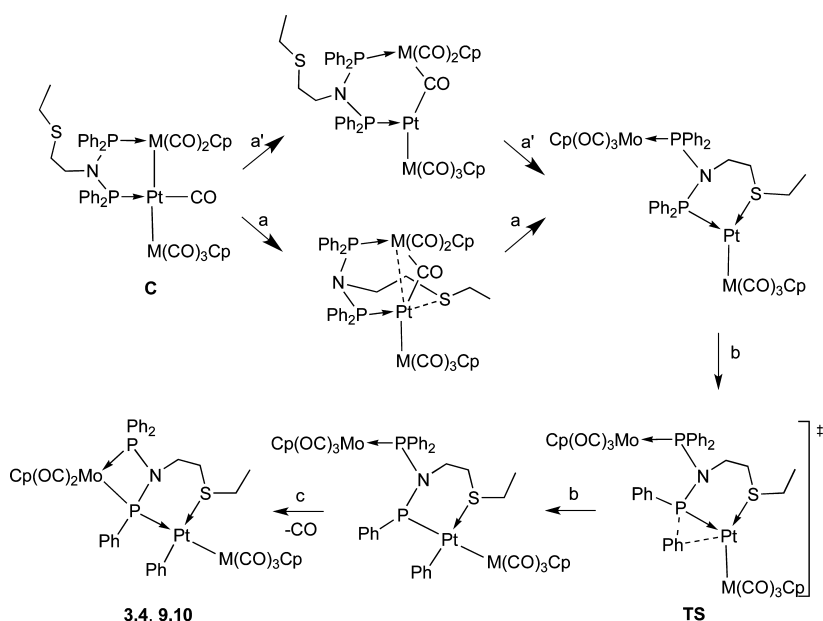
Figure 7. Enthalpy profile for the formation in THF of the dinuclear PtMo species 15, the triangular PtMo₂ clusters 7 (chelated) and 5 (bridged), the foreseen intermediates B–D, and the six-membered platinacycle complex 3 from the mononuclear Pt complex 1 and 1 or 2 equiv of Na[M(CO)₃Cp], according to the mechanism reported in Scheme 8 (data for M = Mo and R' = CH₂CH₂S(CH₂)₅CH₃).

clusters 5,6 and 11,12, the bridged clusters 7,8 and 13,14, and also of the six-membered platinacycle complexes 3,4 and 9,10, resulting from the reaction of the mononuclear Pt complexes 1,2 with 1 or 2 equiv of Na[M(CO)₃Cp].

The relative enthalpies and free energies of the species involved in this mechanism are reported in Table 4, and shown for M = Mo and R = (CH₂)₅CH₃ in Figures 7 and Supporting Information, Figure S18. It is apparent that both chloride substitution steps are exothermic and exoergic and that the six-membered platinacycle complexes are 10–20 kcal mol⁻¹ more stable in free energy than the bridged or chelated trinuclear clusters. Moreover, as already found for the analogous complexes with a simple *n*-decyl chain on the dppa ligand, the linear chain intermediate C is significantly more stable than both isomers of the trinuclear clusters, and to a lesser extent than the six-membered platinacycle complexes, the driving force for their

formation being the entropic gain due to the loss of a CO molecule.

To gain more insight into the mechanism of formation of the six-membered platinacycle complexes 3,4 and 9,10 from the mononuclear Pt complexes 1,2, we performed DFT calculations on several plausible mechanisms envisaged on the basis of the experimental data. It is important to remember that the skeletal rearrangement observed in the formation of these six-membered platinacycle complexes did not occur with the analogous complexes where the dppa ligand is substituted with the *n*-decyl chain, which points to a key role of the sulfur donor in triggering this reaction. Moreover, the failure of an external thioether ligand to facilitate P–C bond activation in a manner similar to that observed for the synthesis of 3,4 and 9,10, indicates the importance of the chelate effect of the potentially tridentate (PSP) ligand which, from a theoretical point of view,

Scheme 9. A Possible Mechanism for the Formation of the Six-Membered Platinacycle Complexes 3, 4, 9, and 10 Starting from Species C^a

^aTwo different pathways can be considered, a or a', see text.

underlines the key role played by entropy in the limiting step of the reaction.

Even with this limitation, several possible reaction mechanisms can be envisaged for the sulfur-triggered phenyl migration leading to the formation of 3–4, 9–10. In principle, the migration could occur starting from (i) the initial reactants 1,2; (ii) the monosubstitution products 15–18; (iii) the chelated trinuclear clusters 5,6, 11,12; (iv) the bridged trinuclear clusters 7,8, 13,14; (v) any of the stable intermediates B–D in Scheme 8; upon intramolecular sulfur attack followed by phenyl migration and further steps and/or rearrangements depending on the starting molecule.

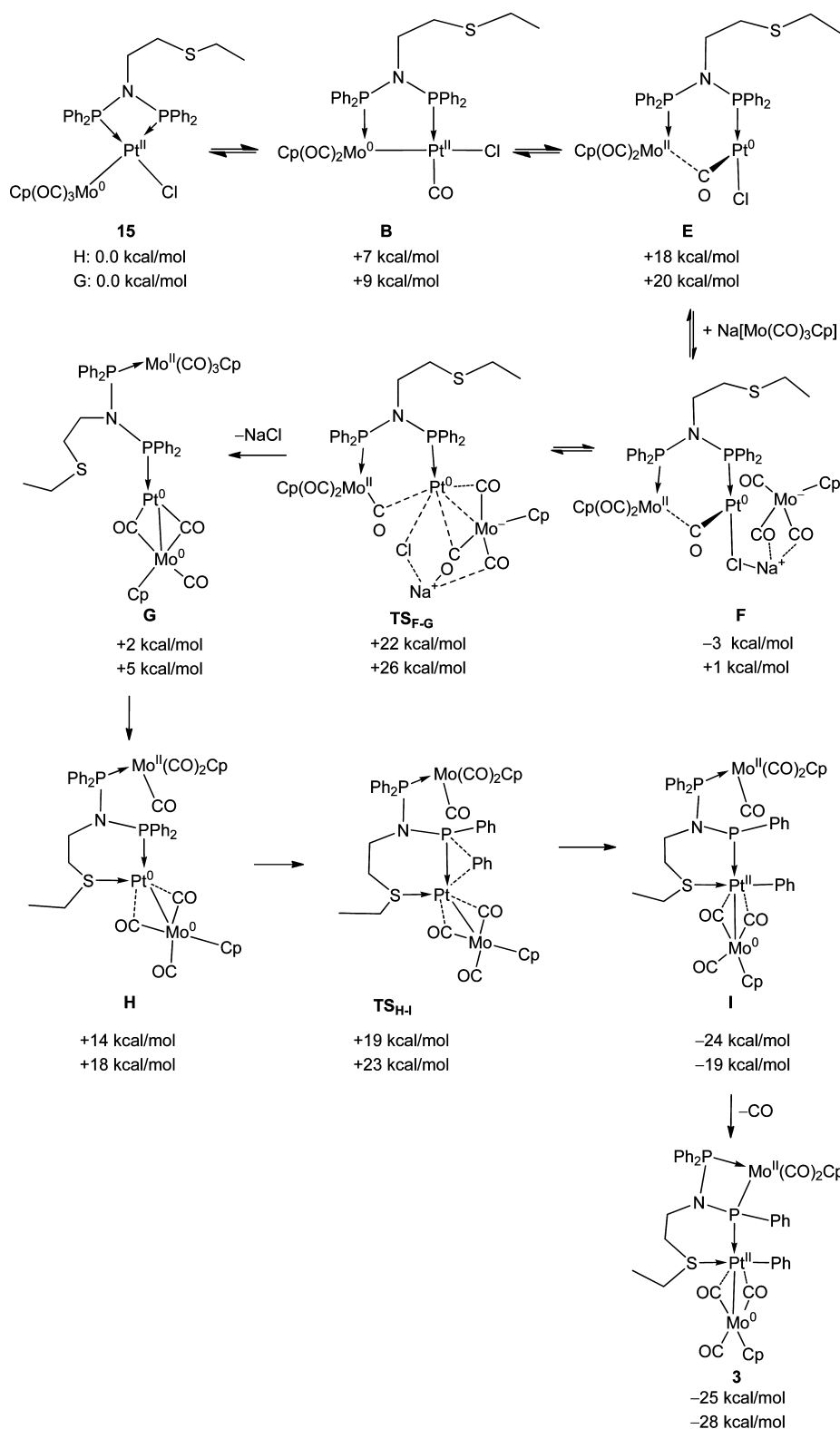
A closer look at the structure of the six-membered platinacycle points out that the two M metals are far apart from each other and that the PNP ligand is bonded to the Pt and to one of the M centers, suggesting as plausible starting species for the phenyl migration a bridged PtM₂ species in which the two M metals are not bound to each other, as in intermediate C. The monosubstitution intermediate B should also be taken into account as starting species for the phenyl migration, provided that the second metalate substitution occurs after phenyl migration. Intermediate C is probably the most plausible candidate for the initial phenyl migration as it is the most stable species identified (see Table 4), and only two additional steps, a Pt–M bond breaking and a CO decoordination, are required for the formation of the six-membered platinacycle. A simple mechanism can be devised starting from C that consists of the following steps: the breaking of the Pt–MP bond, stabilized by a CO bridge between Pt and the P-bound M center, which is assisted (a) or followed (a') by the intramolecular coordination of the sulfur atom to Pt with CO migration from Pt to M; (b) the subsequent phenyl migration from P to the unsaturated Pt center; (c) the final coordination of the P atom already bound to Pt to the Mo center with loss of the M-bound CO, see Scheme 9.

However, preliminary calculations on the breaking of the bond between Pt and the P-substituted M atom, with or without simultaneous intramolecular coordination of the Pt center by the

sulfur atom of the N-substituted dppe ligand, indicated a large energy increase, above 40 kcal/mol, thus ruling out this possibility.

Another candidate for the phenyl migration is the bridged isomer B of the monosubstitution products 15–18, see Scheme 8, with the second metalate substitution occurring after phenyl migration. This possibility is supported by the following experimental evidence: (i) the isolation of the dinuclear PtM species 15–18 upon reaction of 1,2 with only 1 equiv of Na[M(CO)₃Cp]; (ii) the reaction of 3,4, 9,10 with halide sources gives the dinuclear products 21–26, maintaining the same six-membered platinacycle but with the Pt-bound [M(CO)₃Cp] moiety replaced by Cl. After several attempts, we found a plausible inner redox mechanism whereby an initial heterolytic breaking of the Pt–M bond occurs from the bridged isomer B leading to the unstable species E and changing the initial metal formal oxidation states, Pt(II) and M(0), respectively, to Pt(0) and M(II). The shift of the Mo–Pt bond electron pair to the Pt atom upon breaking is testified by the changes of Mulliken charges on the metal atoms (from +0.120 on Pt and +0.040 on Mo in B to –0.070 on Pt and +0.247 on Mo in E), see Supporting Information, Table S1. This process is assisted by the approach of a second sodium metalate with the substitution of the chloride on Pt. The mechanism proceeds with (i) the intramolecular coordination of the sulfur atom of the N-substituted dppe ligand to the coordinatively unsaturated Pt(0) center and (ii) the P to Pt phenyl migration, and is completed (iii) by the coordination of the P atom previously bound to Pt to the M center (Scheme 10). The key step for the P to Pt phenyl migration can be viewed as a P–Ph oxidative addition to the metal center, which is favored by a transiently formed Pt(0) species and by the lengthening of one of the carbonyl–Mo^{II} bond.

A careful scrutiny by DFT calculations for M = Mo confirmed the feasibility of such a mechanism. Calculations were performed on the intermediate B and on all the species involved in each of

Scheme 10. Proposed Mechanism for the Formation of the Six-Membered Platinacycles Products^a

^aEnthalpies and free energies (in kcal mol⁻¹) are reported for the compounds with M = Mo and R = (CH₂)₅CH₃ in THF.

the above steps, including the identification of possible transition states for the key steps, and the evaluation of all their energies.

The calculated enthalpies and free energies of all the intermediates and main transition states involved in this mechanism are reported in Scheme 10 and Figure 8 for M = Mo and

R = (CH₂)₅CH₃ and show that the highest barrier corresponds to the breaking of the Pt–Mo bond with a value of 22 kcal·mol⁻¹ in enthalpy (26 kcal·mol⁻¹ in free energy). The height of these barriers indicates a very slow kinetics at room temperature, which is consistent with the occurrence of this reaction at 323 K but not

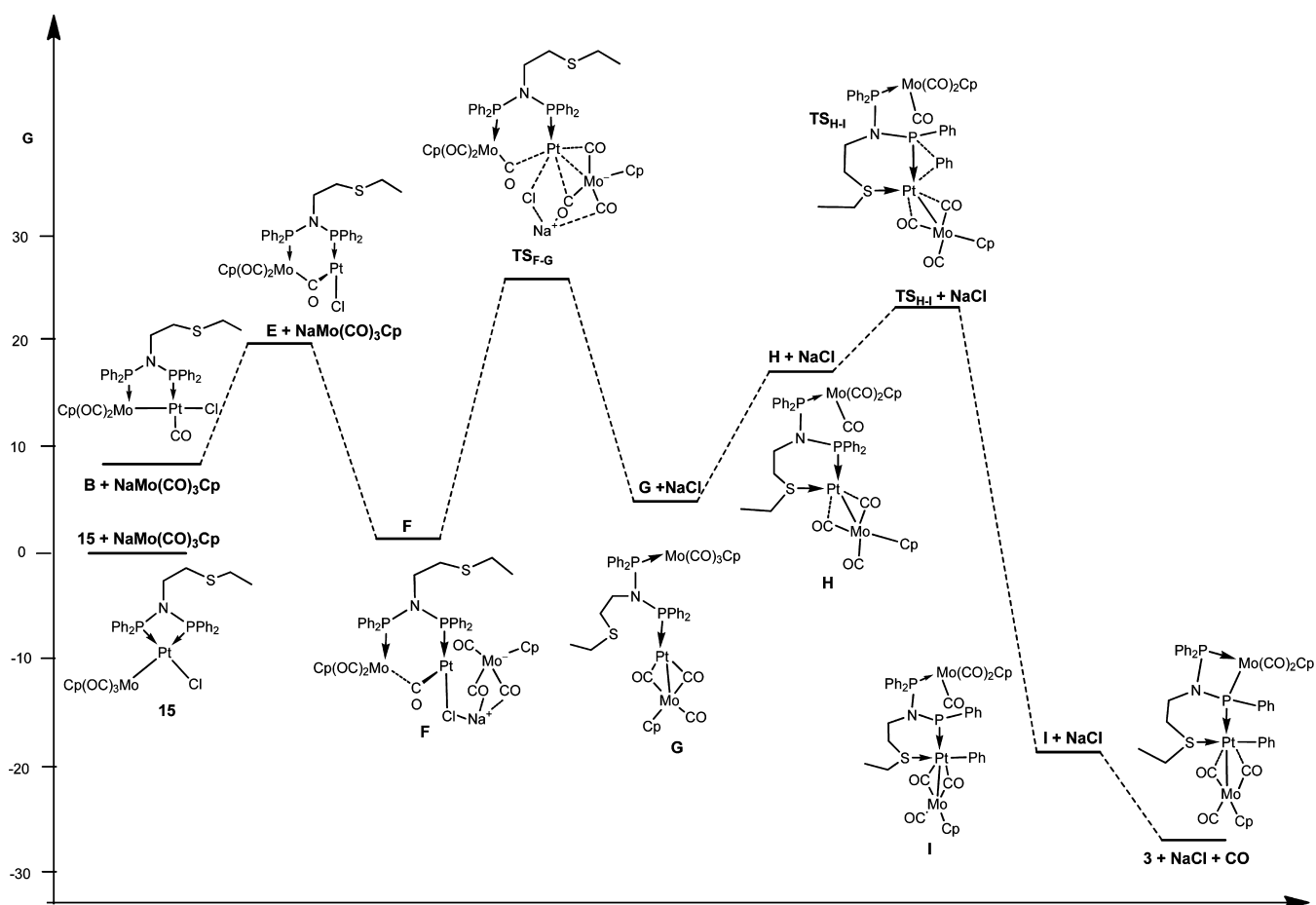


Figure 8. Free energy profile (in $\text{kcal}\cdot\text{mol}^{-1}$), in THF, for the formation of the six-membered platincyclus product **3** from intermediate **B**, according to the mechanism of Scheme 10.

at 273 K. In fact, performing the reactions of **1** or **2** with $\text{Na}[\text{M}(\text{CO})_3\text{Cp}]$ at 273 K in THF afforded, after 24 h, only the monosubstituted species **15**–**18**.

It is worth noting that the highest minimum in the potential energy surface from which the phenyl migration is triggered, **H**, is a rather unstable species with platinum already coordinated by the sulfur atom and a carbonyl group of the P-bound Mo unit loosely bonded to M (calculated C–Mo distance = 2.283 Å). Its structure is quite close to the corresponding transition state as is its energy, only 5 $\text{kcal}\cdot\text{mol}^{-1}$ below in enthalpy (5 $\text{kcal}\cdot\text{mol}^{-1}$ in free energy). The driving force for the migration of the phenyl cation can be therefore the increased negative charge borne by the Pt(0) metal center upon S coordination ($-0.08 e$). The phenyl migration also leads to a significant increase of the metal charge (+0.12 e) in line with the proposed increase of the Pt formal oxidation number from 0 in **H** to +2 in **I** (see Mulliken charges in Supporting Information, Table S1).

To substantiate the mechanism proposed by DFT calculations, we monitored by $^{31}\text{P}\{^1\text{H}\}$ NMR THF solutions of **1** or **2** to which $\text{Na}[\text{Mo}(\text{CO})_3\text{Cp}]$ or $\text{Na}[\text{W}(\text{CO})_3\text{Cp}]$ were successively added at 323 K. Figure 9 shows the course of the reaction between **2** and $\text{Na}[\text{Mo}(\text{CO})_3\text{Cp}]$. It is apparent that in the early stage of the reaction (1 equiv of $\text{Na}[\text{Mo}(\text{CO})_3\text{Cp}]$ added), the starting material is converted into the monochlorido species **16**, which, as soon as it accumulates in solution, evolves toward the phosphanido-bridged complex **4**, which constitutes the major reaction product, along with the chelate species **6** and the bridged cluster **8**. After 2.2 equiv of $\text{Na}[\text{Mo}(\text{CO})_3\text{Cp}]$ were added, the

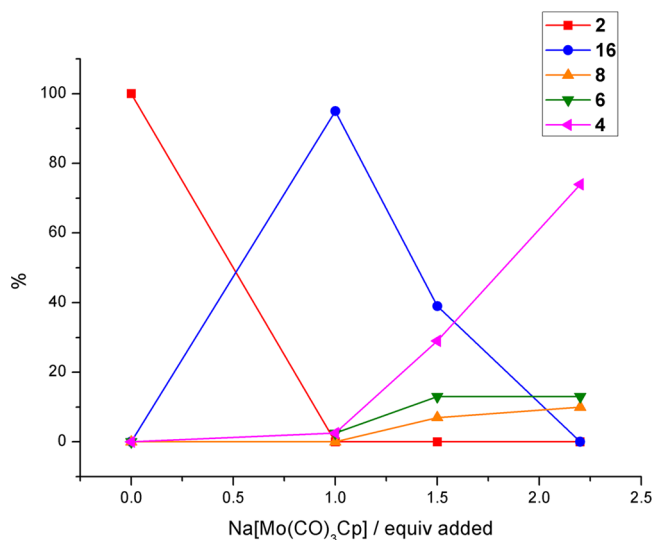


Figure 9. Course of the reaction between **2** and $\text{Na}[\text{Mo}(\text{CO})_3\text{Cp}]$.

reaction solution contained $\sim 70\%$ of **4**, along with 13% of **6** and 10% of **8**, plus other unidentified decomposition compounds. Prolonged reaction times resulted only in extensive decomposition of **6** and **8**. The monitoring of the reaction between **1** and $\text{Na}[\text{Mo}(\text{CO})_3\text{Cp}]$ gave comparable results (Supporting Information, Figure S19). In the case of the tungsten species, the reaction is less selective toward the formation of the

corresponding phosphanido-bridged complexes, and the decomposition of the chelate and bridged species at long reaction times is more pronounced. The solution obtained after addition of 2.2 equiv of $\text{Na}[\text{W}(\text{CO})_3\text{Cp}]$ to **1** (Figure 10) contained $\sim 34\%$

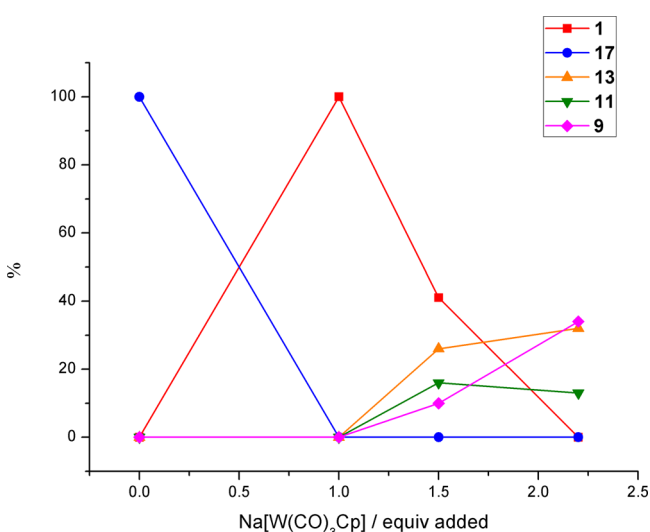


Figure 10. Course of the reaction between **1** and $\text{Na}[\text{W}(\text{CO})_3\text{Cp}]$.

of the phosphanido-bridged complex **9**, along with 32% of **13** and 12% of **11**, plus other unidentified decomposition compounds. The monitoring of the reaction between **2** and $\text{Na}[\text{W}(\text{CO})_3\text{Cp}]$ gave comparable results (Supporting Information, Figure S20).

The contemporary formation of chelate, bridged, and phosphanido-bridged species observed during reaction monitoring suggests that the chelate and bridged species are not precursors to the phosphanido-bridged complexes, in accord with the DFT mechanism.

Another clue to the mechanism proposed by DFT methods stemmed from the sequential reaction of **2** with first $\text{Na}[\text{Mo}(\text{CO})_3\text{Cp}]$ and then $\text{Na}[\text{W}(\text{CO})_3\text{Cp}]$. For this experiment, to a THF solution of **2** kept at 323 K was added 1.0 equiv of $\text{Na}[\text{Mo}(\text{CO})_3\text{Cp}]$, causing the formation of the monochlorido complex **16** (90%) plus minor amounts of **4**, **6**, and **8**. The subsequent addition of 1.0 equiv of $\text{Na}[\text{W}(\text{CO})_3\text{Cp}]$ resulted in the formation of a new species, in ca. 60% spectroscopic yield,⁶⁰ characterized by two doublets at δ 90.1 and δ 73.0 ($J_{\text{P,P}} = 68$ Hz)

in the $^{31}\text{P}\{^1\text{H}\}$ NMR spectrum and by a doublet centered at δ -3599 in the $^{195}\text{Pt}\{^1\text{H}\}$ NMR spectrum. The absence of ^{183}W satellites for the $^{31}\text{P}\{^1\text{H}\}$ NMR signals, together with the similarity of $^{195}\text{Pt}\{^1\text{H}\}$ NMR chemical shift with that of the PtW_2 complex **10** (δ -3605), indicate that the new species is the phosphanido bridged complex **31** in which a Mo atom is chelated by the two P atoms, and a W atom is bonded to Pt (Scheme 11).⁶¹

The formation of **31** indicates that of the 2 equiv of metalate necessary to form the phosphanido-bridged species **3**, **4**, **9**, and **10**, the first one contains the metal atom to become chelated by the two P atoms (M^1 in Scheme 2), and the second one contains the metal atom bonded to platinum (i.e., M^2 in Scheme 2) in the final products. This is in accord with the mechanism outlined in Scheme 10, where the Mo chelated by the two P atoms arises from the Mo present in the monochlorido species **15**, while the Mo atom bound to Pt in the final products originates from the second equivalent of metalate. The formation of the phosphanido-bridged complex **30** in which a W atom is chelated by the two P atoms, and a Mo atom is bonded to Pt (see headings of Table 4), was detected by performing the sequential reaction of **2** with first $\text{Na}[\text{W}(\text{CO})_3\text{Cp}]$ and then $\text{Na}[\text{Mo}(\text{CO})_3\text{Cp}]$. However, the addition of $\text{Na}[\text{Mo}(\text{CO})_3\text{Cp}]$ to a solution containing mostly the monochlorido complex **17** led to a partial substitution of the Mo for the W yielding **16**. The reaction of **16** and **17**, contemporarily present in solution together with $\text{Na}[\text{Mo}(\text{CO})_3\text{Cp}]$ and $\text{Na}[\text{W}(\text{CO})_3\text{Cp}]$, afforded **31** (18%), **4** (14%), and **10** (14%), besides **30** (17%)⁶² (see Table 5 for the associated NMR features).

3. CONCLUSIONS

A major result from this work has been the demonstration that the presence of a thioether function in the N-substituent of dppa-type ligands chelated to Pt(II) complexes dramatically influences the nature of the reaction products with carbonylmetalates such as $[\text{Mo}(\text{CO})_3\text{Cp}]^-$ or $[\text{W}(\text{CO})_3\text{Cp}]^-$. This unexpected influence was clearly demonstrated by comparison with similar reactions performed with dppa-type ligands having a N-substituent alkyl chain of similar length than the thioether group. Whereas in both cases formation of the expected Pt–M bonds was observed, only when the thioether function was present did we observe a thermally induced transfer of a phenyl group from a PPh_2 group to platinum. Furthermore, it was shown that the corresponding P–C bond activation reaction could be

Scheme 11. Sequential Reaction of **2** with First $\text{Na}[\text{W}(\text{CO})_3\text{Cp}]$ and Then $\text{Na}[\text{Mo}(\text{CO})_3\text{Cp}]$

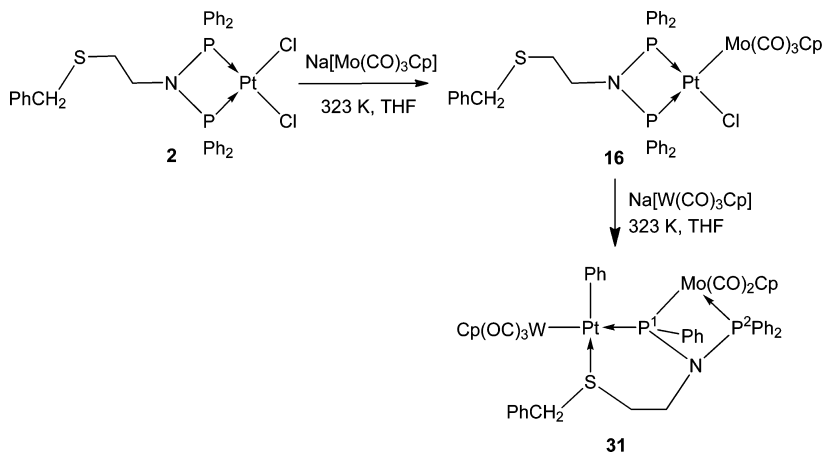
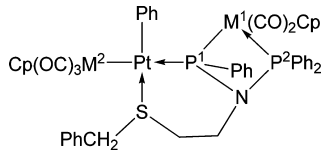


Table 5. $^{31}\text{P}\{^1\text{H}\}$ NMR Features of the Trinuclear Complexes **4**, **10**, **30**, and **31** (THF, 298 K)


compound	M ¹	M ²	δ P ¹ , ppm	δ P ² , ppm	$^2J_{\text{P,P}}$, Hz	$^1J_{\text{P,Pt}}$, Hz	δ Pt, ppm
4	Mo	Mo	88.7	73.1	68	2819	-3517
10	W	W	60.0	41.5	55	2875	-3605
30	W	Mo	58.1	41.5	57	2811	-3514
31	Mo	W	90.1	73.0	68	2798	-3599

made reversible upon oxidation with iodine or protonation. Such thermally or chemically triggered transformations in heterometallic complexes are relevant not only to the synthesis of novel architectures but also to elementary steps that may occur under catalytic conditions. Furthermore, they provide direct evidence for the occurrence of synergistic effects in polynuclear complexes, in particular, in heterometallic systems. Spectroscopic and/or structural investigations by X-ray diffraction have established the nature of the complexes described in this work and a theoretical study by DFT methods has allowed us to suggest mechanistic pathways for the transformations observed experimentally.

4. EXPERIMENTAL SECTION

All manipulations were conducted under an inert gas (argon) using standard Schlenk techniques. Solvents were dried and distilled under argon according to standard procedures.

Multinuclear NMR spectra were recorded with a Bruker Avance 400 spectrometer (400 MHz for ^1H) at 298 K; chemical shifts are reported in parts per million referenced to SiMe_4 for ^1H and ^{13}C , to H_3PO_4 for ^{31}P , and to H_2PtCl_6 for ^{195}Pt . The signal attributions and coupling constant assessment was made on the basis of a multinuclear NMR analysis including, beside one-dimensional spectra, $^{31}\text{P}\{^1\text{H}\}$ COSY, ^1H COSY, ^1H NOESY, $^1\text{H}-^{13}\text{C}$ HMQC, $^1\text{H}-^{13}\text{C}$ HMBC, $^1\text{H}-^{31}\text{P}$ HMQC, $^1\text{H}-^{195}\text{Pt}$ HMQC. The IR spectra were recorded with Bruker Vector 22 or Jasco FT-IR-4200 spectrometers. High-resolution mass spectrometry (HRMS) and MS/MS analyses were performed using a time-of-flight mass spectrometer equipped with an electrospray ion source (Bruker micrOTOF-Q II). The analyses were performed in a positive ion mode. The sample solutions were introduced by continuous infusion with the aid of a syringe pump at a flow rate of 180 $\mu\text{L}/\text{h}$. The instrument was operated at end plate offset -500 V and capillary -4500 V. Nebulizer pressure was 0.3 bar (N_2), and the drying gas (N_2) flow was 4 L/min. Drying gas temperature was set at 453 K. The software used for the simulations is Bruker Daltonics DataAnalysis (version 4.0). C, H, and N elemental analyses were performed with a Eurovector CHNS-O EA3000 Elemental Analyzer. Cl elemental analysis was performed by potentiometric titration using a Metrohm DMS Titrino. The complexes $[\text{PtCl}_2\{(\text{Ph}_2\text{P})_2\text{N}(\text{CH}_2\text{CH}_2\text{SR})\text{-PP}\}]$ [$\text{R} = \text{CH}_2\text{C}_6\text{H}_5$, $(\text{CH}_2)_5\text{CH}_3$], $[\text{PtL}_2(\text{cod})]$, $^{63}\text{Na}[\text{M}(\text{CO})_3\text{Cp}]$ ($\text{M} = \text{Mo}, \text{W}$, as 1,2-dimethoxyethane solvates), 64 and the diphosphanylamine $(\text{Ph}_2\text{P})_2\text{N}(\text{CH}_2)_2\text{SCH}_2\text{Ph}$ 68 were prepared by literature methods. Gaseous HCl was prepared by action of concentrated sulfuric acid on solid NaCl.

X-ray Crystallography. 65 Crystal data, parameters for intensity data collection, and convergence results for **9** and **4** are compiled in Table 6. Diffraction-quality crystals were obtained by slow diffusion of *n*-hexane into THF solutions of the compounds. Data were collected with Mo $K\alpha$ radiation ($\lambda = 0.71073$ Å) on a Bruker D8 goniometer with SMART CCD area detector; radiation sources were a sealed tube for the intensity data of **4** and an INCOATEC microsource with multilayer optics in the case of **9**. Multiscan-based absorption corrections were performed with the help of the program SADABS. 66 The structures were

Table 6. Crystallographic Data and Structural Refinement Details for **9** and **4**

	9	4
empirical formula	$\text{C}_{49}\text{H}_{51}\text{NO}_{5.5}\text{P}_2\text{PtSW}_2$	$\text{C}_{48}\text{H}_{41}\text{Mo}_2\text{NO}_5\text{P}_2\text{PtS}$
formula mass	1398.70	1192.79
temperature [K]	100(2)	193(2)
approx. crystal dimensions [mm]	$0.17 \times 0.03 \times 0.03$	$0.3 \times 0.3 \times 0.2$
wavelength [Å]	0.71073	0.71073
crystal system	triclinic	triclinic
space group	$P\bar{1}$	$P\bar{1}$
unit cell dimensions		
<i>a</i> [Å]	11.5033(8)	8.9112(9)
<i>b</i> [Å]	13.1859(9)	12.4727(13)
<i>c</i> [Å]	16.4015(11)	20.138(2)
α [deg]	68.7160(10)	87.646(2)
β [deg]	77.7450(10)	87.333(2)
γ [deg]	78.5260(10)	80.118(2)
<i>V</i> [Å ³]	2244.9(3)	2201.4(4)
<i>Z</i>	2	2
<i>D</i> _{calcd.} [Mg m ⁻³]	2.069	1.799
absorption coeff. [mm ⁻¹]	8.387	3.899
θ range for data coll. [deg]	1.67 to 28.60	2.32 to 27.04
collected reflections	40 879	27 717
independent reflections (<i>R</i> _{int})	11 373 (0.0883)	9563 (0.0575)
data/parameters	11 373/549	9563/541
GOF on <i>F</i> ²	0.995	1.005
<i>R</i> ^a (<i>I</i> > 2 σ (<i>I</i>))	0.0395	0.0398
<i>wR</i> ₂ ^b (all data)	0.0792	0.0644
largest diff. peak/hole [e ⁻ Å ⁻³]	2.840–2.512	1.243–0.668

$$^a R = \sum ||F_o| - |F_c|| / \sum |F_o|. \quad ^b wR_2 = [\sum w(F_o^2 - F_c^2)^2 / \sum w(F_o^2)^2]^{1/2}.$$

solved by direct methods and refined with full-matrix least-squares on F^2 .⁶⁷ A total of 77 rigid-bond restraints⁶⁸ were employed in the refinement of **9** to ensure physically acceptable displacement parameters.

Synthesis of the Monosubstituted Complexes 15–18. An acetonitrile solution (7 mL) of Na[Mo(CO)₃Cp]·2DME (69 mg, 0.155 mmol; DME = 1,2-dimethoxyethane) was added dropwise to a stirred solution of **1** (95 mg, 0.146 mmol) in acetonitrile (3.0 mL) and kept at 323 K. The pale yellow solution turned immediately orange, and after it was stirred for 1 h, the mixture was cooled; analysis by NMR and HRMS revealed the quantitative transformation into **15** (spectroscopic yield >95%). Removal of the solvent and treatment with toluene to purify the product resulted in partial conversion of **15** into **5**+**7** due to the slight excess of metalate used. The same procedure was followed for the synthesis of **16–18**. The atom numbering of the sketch in Chart 1 was used for the NMR characterization.

Synthesis of 3. A THF solution (25 mL) of Na[Mo(CO)₃Cp]·2DME (148 mg, 0.33 mmol) was added dropwise within 40 min to a stirred solution of **1** (150 mg, 0.15 mmol) in THF (3.0 mL) kept at 323 K. The pale yellow solution darkened, and after it was stirred for 4 h, the mixture was cooled to room temperature and the solvent was removed under reduced pressure. Toluene (30 mL) was added to the residue, and the resulting suspension was filtered. The filtrate was evaporated, and the residue was washed with methanol (2 × 5 mL). Pure **3** was obtained as a dark yellow solid by crystallization from THF/*n*-hexane. Yield: 55%. Anal. Calcd for C₄₇H₄₇Mo₃NO₃P₂PtS⁺ (**3**): C 47.56, H 3.99, N 1.18; Found C 47.61, H 3.94, N 1.12%. HRMS(+) in MeCN/MeOH (collision energy = 10 eV), exact mass for the cation [C₃₉H₄₀MoNO₃P₂PtS]⁺: 942.1110; measured: m/z : 942.1143 [M−{Mo(CO)₃Cp}]⁺. HRMS(+) in acetone (collision energy = 2 eV), exact mass for the cation [C₅₁H₅₆NO₆P₂PtSMo₂]⁺: 1188.0492 da; measured m/z : 1188.0368 [M + H]⁺. IR ν_{CO} (KBr)/cm⁻¹: 1779 (vs), 1798 (vs), 1898 (sh), 1889 (vs), 1977 (sh), 1970 (vs); ν_{CO} (THF)/cm⁻¹: 1788 (vs), 1894 (vs), 1975 (vs).

¹H NMR (C₆D₆, 298 K): δ 8.80 (dd, ³J_{H,P} = 10 Hz, ³J_{H,H} = 8 Hz, 2H, ortho H_{ringB}), 7.99 (ddd, ³J_{H,P} = 11 Hz, ³J_{H,H} = 8 Hz, ⁴J_{H,H} = 1 Hz, 2H, ortho H_{ringC}), 7.91 (d, ³J_{H,H} = 7 Hz, ³J_{H,P} = 50 Hz, 2H, ortho H_{ringA}), 7.42 (overlapped, 2H, meta H_{ringC}), 7.41 (overlapped, 2H, ortho H_{ringD}), 7.39 (overlapped, 2H, meta H_{ringB}), 7.26 (pseudo td, ³J_{H,H} = 7 Hz, ⁴J_{H,P} = 2 Hz, 2H, meta-H_{ringD}), 7.16 (overlapped, 1H, para H_{ringD}), 7.14 (overlapped, 1H, para H_{ringC}), 7.07 (t, 1H, para-H_{ringB}), 6.87 (t, ³J_{H,H} = 7 Hz, 2H, meta-H_{ringA}), 6.71 (t, ³J_{H,H} = 7 Hz, 1H, para-H_{ringA}), 4.87 (s, 5 H, Cp-Mo¹), 4.50 (s, 5 H, Cp-Mo²), 3.09 (ddd, 1H, ²J_{H,H} = 16 Hz, ³J_{H,H} = 9 Hz, ³J_{H,H} = 6 Hz, C₅H₁₁HCH-S), 2.86 (m, 1H, HCH-N), 2.67 (m, 1H, HCH-N), 2.35 (ddd, 1H, ²J_{H,H} = 14 Hz, ³J_{H,H} = 10 Hz, ³J_{H,H} = 4 Hz, C₅H₁₁HCH-S), 1.87 (ddd, 1H, ²J_{H,H} = 14 Hz, ³J_{H,H} = 8 Hz, ³J_{H,H} = 2 Hz, S-HCHCH₂N), 1.77 (ddd, 1H, ²J_{H,H} = 14 Hz, ³J_{H,H} = 7 Hz, ³J_{H,H} = 2 Hz, S-HCHCH₂N), 1.37–0.99 (8 H, alkyl protons), 0.82 (t, ³J_{H,H} = 7 Hz, 3H, CH₃). ¹³C{¹H} APT (THF-*d*₈, 298 K): δ 240.5 (d, $J_{C,P}$ = 25 Hz, CO), 238.6 (d, $J_{C,P}$ = 26 Hz, CO), 237.0 (br, CO), 235.3 (br, CO), 235.2 (br, CO), 143.7 (br, C_{ipso}), 142.1 (d, br, $J_{C,P}$ = 7 Hz, C_{ipso}), 137.5 (d, $J_{C,P}$ = 37 Hz, C_{ipso}), 133.5 (d, $J_{C,P}$ = 13 Hz, C_{ph}), 132.9 (d, $J_{C,P}$ = 47 Hz, C_{ipso}), 131.7 (d, $J_{C,P}$ = 12 Hz, C_{ph}), 131.2 (d, $J_{C,P}$ = 2 Hz, C_{ph}), 131.0 (d, $J_{C,P}$ = 12 Hz, C_{ph}), 130.8 (d, $J_{C,P}$ = 2 Hz, C_{ph}), 129.3 (s, C_{ph}), 129.2 (s, C_{ph}), 129.1 (s, C_{ph}), 128.8 (d, $J_{C,P}$ = 11 Hz, C_{ph}), 127.9 (s, C_{ph}), 127.8 (s, C_{ph}), 121.3 (s, C_{ph}), 92.7 (s, C_{Cp-Mo2}), 90.6 (s, C_{Cp-Mo1}), 46.4 (br, CH₂N), 33.4 (s, C₅H₁₁CH₂S), 31.7 (s, C_{Alk}), 31.3 (s, C_{Alk}), 29.9 (s, C_{Alk}), 27.2 (s, CH₂CH₂N), 22.6 (s, C_{Alk}), 13.6 (s, CH₃). ³¹P{¹H} NMR (THF-*d*₈, 298 K): δ 88.7 (d, ²J_{P,P} = 68 Hz, ¹J_{P,Pt} = 2849 Hz, P¹), 73.2 (d, ²J_{P,P} = 68 Hz, P²). ¹⁹⁵Pt{¹H} NMR (THF-*d*₈, 298 K): δ −3508 (broad d, ¹J_{P,Pt} = 2849).

Synthesis of 4. Complex **4** was prepared by following the same procedure used for **3**, starting from Na[Mo(CO)₃Cp]·2DME (147 mg, 0.33 mmol) and **2** (119 mg, 0.15 mmol). Yield: 71%. Anal. Calcd for C₄₈H₄₁Mo₂NO₃P₂PtS: C 48.33, H 3.46, N 1.17; found C 48.28, H 3.49, N 1.11%. HRMS(+) in MeCN/MeOH (collision energy = 10 eV), exact mass for the cation [C₄₀H₃₆MoNO₂P₂PtS]⁺: 948.0641; measured: m/z : 948.0653 [M−{Mo(CO)₃Cp}]⁺. HRMS(+) in acetone (collision energy = 2 eV), exact mass for the cation [C₄₈H₄₁Mo₂NO₃P₂PtS]⁺: 1192.9944 da; measured m/z : 1192.9973 [M]⁺. IR ν_{CO} (KBr)/cm⁻¹: 1785 (vs), 1801 (vs), 1873 (vs), 1896 (vs), 1965 (vs), 1974 (vs);

ν_{CO} (THF)/cm⁻¹: 1792 (vs), 1894 (vs), 1976 (vs). ¹H NMR (THF-*d*₈, 298 K): δ 8.49 (ddd, ³J_{H,P} = 11 Hz, ³J_{H,H} = 8 Hz, ⁴J_{H,H} = 1 Hz, 2H, ortho H_{ringB}), 7.96 (ddd, ³J_{H,P} = 11 Hz, ³J_{H,H} = 8 Hz, ⁴J_{H,H} = 1 Hz, 2H, ortho H_{ringC}), 7.56 (overlapped, 6H, ortho H_{ringD} + ortho H_{ringA} + meta H_{ringC}), 7.50 (overlapped, 1H, para H_{ringC}), 7.43 (pseudo t, ³J_{H,H} = 8 Hz, 2H, meta-H_{ringB}), 7.33 (overlapped, 3H, meta H_{ringD} + para-H_{ringB}), 7.17 (m, 1H, para H_{ringD}), 7.06 (m, 3H, meta + para-H_{benzyl ring}), 6.91 (m, 2H, ortho-H_{benzyl ring}), 6.83 (broad, 2H, meta-H_{ringA}), 6.67 (td, ³J_{H,H} = 7 Hz, ⁴J_{H,H} = 1 Hz, 1H, para-H_{ringA}), 4.79 (d, ⁴J_{H,P} = 0.6 Hz, 5 H, Cp-Mo¹), 4.73 (s, 5 H, Cp-Mo²), 4.03 (d, ²J_{H,H} = 14 Hz, 1 H, C₆H₅HCH-S), 3.28 (d, ²J_{H,H} = 14 Hz, C₆H₅HCH-S), 3.20 (m, 1H, HCH-N), 3.03 (m, 1H, HCH-N), 1.93 (m, 1H, S-HCHCH₂N), 1.81 (m, 2H, S-HCHCH₂N). ¹³C{¹H} APT (THF-*d*₈, 298 K): δ 240.2 (d, $J_{C,P}$ = 26 Hz, CO), 238.4 (d, $J_{C,P}$ = 26 Hz, CO), 237.7 (br, CO), 235.2 (br, CO), 235.0 (br, CO), 144.1 (br, C_{ipso}), 142.4 (d, br, $J_{C,P}$ = 7 Hz, C_{ipso}), 136.9 (d, $J_{C,P}$ = 38 Hz, C_{ipso}), 135.2 (s, C_{ipso}), 133.3 (d, $J_{C,P}$ = 14 Hz, C_{ph}), 132.5 (d, $J_{C,P}$ = 47 Hz, C_{ipso}), 131.6 (d, $J_{C,P}$ = 11 Hz, C_{ph}), 131.0 (d, $J_{C,P}$ = 2 Hz, C_{ph}), 130.8 (d, $J_{C,P}$ = 10 Hz, C_{ph}), 130.7 (d, $J_{C,P}$ = 3 Hz, C_{ph}), 129.3 (s, C_{ph}), 129.2 (d, $J_{C,P}$ = 2 Hz, C_{ph}), 129.0 (d, $J_{C,P}$ = 10 Hz, C_{ph}), 128.7 (d, $J_{C,P}$ = 10 Hz, C_{ph}), 128.3 (s, C_{ph}), 128.1 (s, C_{ph}), 127.8 (s, C_{ph}), 127.7 (s, C_{ph}), 127.4 (s, C_{ph}), 121.4 (s, C_{ph}), 92.4 (s, C_{Cp-Mo2}), 90.6 (s, C_{Cp-Mo1}), 46.3 (s, CH₂N), 38.3 (s, PhCH₂S), 25.5 (s, S-CH₂CH₂N). ³¹P{¹H} NMR (THF-*d*₈, 298 K): δ 88.7 (d, ²J_{P,P} = 68 Hz, ¹J_{P,Pt} = 2819 Hz, P¹), 73.1 (d, ²J_{P,P} = 68 Hz, P²). ¹⁹⁵Pt{¹H} NMR (THF-*d*₈, 298 K): δ −3517 (broad d, ¹J_{P,Pt} = 2819 Hz)

Synthesis of 9. Complex **9** was prepared using the same procedure as for **3**, starting from Na[W(CO)₃Cp]·2DME (177 mg, 0.33 mmol) and **1** (121 mg, 0.15 mmol). Yield: 36%. Anal. Calcd for C₅₁H₅₅NO₆P₂PtSW₂ (9·0.5 THF) C 42.08, H 3.68, N 1.00; Found C 42.55, H 3.92, N 0.95%. HRMS(+) in THF/MeOH (collision energy = 10 eV), exact mass for the cation [C₄₀H₃₆NO₂P₂PtSW]⁺: 1028.1499; measured: m/z : 1028.1600 [M−{W(CO)₃Cp}]⁺. HRMS(+) in THF/MeOH (collision energy = 2 eV), exact mass for the cation [C₄₇H₄₇NNaO₅P₂PtSW₂]⁺: 1386.1229 da; measured m/z : 1386.1279 [M + Na]⁺. IR ν_{CO} (KBr)/cm⁻¹: 1773 (vs), 1796 (vs), 1879 (vs), 1889 (vs), 1961 (vs, broad); ν_{CO} (THF)/cm⁻¹: 1786 (vs), 1885 (vs), 1967 (vs). ¹H NMR (THF-*d*₈, 298 K): δ 8.41 (ddd, ³J_{H,P} = 11 Hz, ³J_{H,H} = 7 Hz, ⁴J_{H,H} = 1 Hz, 2H, ortho H_{ringB}), δ 7.96 (ddd, ³J_{H,P} = 11 Hz, ³J_{H,H} = 7 Hz, ⁴J_{H,H} = 1 Hz, 2H, ortho H_{ringC}), 7.58 (overlapped, 2H, meta H_{ringC}), 7.55 (overlapped, 2H, ortho H_{ringD}), 7.51 (overlapped, 2H, meta H_{ringD}), 7.49 (overlapped, 1H, para H_{ringC}), 7.44 (overlapped, 3H, ortho H_{ringA} + para H_{ringD}), 7.35 (pseudo td, ³J_{H,H} = 7 Hz, ⁴J_{H,P} = 1 Hz, 2H, meta-H_{ringB}), 7.23 (td, ³J_{H,H} = 7 Hz, ⁴J_{H,P} = 1 Hz, 1 H, para-H_{ringB}), 6.77 (broad, 2H, meta-H_{ringA}), 6.62 (td, ³J_{H,H} = 7 Hz, ⁴J_{H,P} = 1 Hz, 1H, para-H_{ringA}), 4.92 (s, 5 H, Cp-W¹), 4.75 (s, 5 H, Cp-W²), 3.22 (m, 1H, HCH-N), 3.01 (m, 1H, HCH-N), 2.73 (ddd, 1H, ²J_{H,H} = 16 Hz, ³J_{H,H} = 10 Hz, ³J_{H,H} = 6 Hz, C₅H₁₁HCHS), 2.37 (m, 2H, HCHCH₂N), 2.24 (ddd, 1H, ²J_{H,H} = 16 Hz, ³J_{H,H} = 10 Hz, ³J_{H,H} = 6 Hz, C₅H₁₁HCHS), 1.43–1.05 (8 H, alkyl protons), 0.79 (t, ³J_{H,H} = 7 Hz, 3 H, CH₃). ¹³C{¹H} APT (THF-*d*₈, 298 K): δ 232.0 (d, $J_{C,P}$ = 20 Hz, CO), δ 230.7 (d, $J_{C,P}$ = 20 Hz, CO), δ 230.3 (br, CO), 229.4 (br, CO), 227.1 (br, CO), 143.7 (d, br, $J_{C,P}$ = 9 Hz, C_{ipso}), 142.4 (d, br, $J_{C,P}$ = 7 Hz, C_{ipso}), 138.7 (d, $J_{C,P}$ = 43 Hz, C_{ipso}), 135.5 (d, $J_{C,P}$ = 15 Hz, C_{ph}), 133.5 (d, $J_{C,P}$ = 50 Hz, C_{ipso}), 133.0 (d, $J_{C,P}$ = 13 Hz, C_{ph}), 132.8 (d, $J_{C,P}$ = 12 Hz, C_{ph}), 132.5 (s, C_{ph}), 132.3 (s, C_{ph}), 130.7 (s, C_{ph}), 130.5 (s, C_{ph}), 130.4 (s, C_{ph}), 130.0 (d, $J_{C,P}$ = 10 Hz, C_{ph}), 129.1 (s, C_{ph}), 129.0 (s, C_{ph}), 122.7 (s, C_{ph}), 93.0 (s, C_{Cp-W2}), 90.7 (s, C_{Cp-W1}), 48.4 (br, CH₂N), 34.9 (s, C₅H₁₁CH₂S), 32.8 (s, C_{Alk}), 31.2 (s, C_{Alk}), 29.9 (s, C_{Alk}), 27.4 (br, CH₂CH₂N), 23.9 (s, C_{Alk}), 14.9 (s, CH₃). ³¹P{¹H} NMR (THF-*d*₈, 298 K): δ 59.0 (d, ²J_{P,P} = 55 Hz, ¹J_{P,Pt} = 2904 Hz, ¹J_{P,W} = 158 Hz, P¹), 39.9 (d, ²J_{P,P} = 55 Hz, ¹J_{P,W} = 231 Hz, ³J_{P,Pt} = 23 Hz, P²). ¹⁹⁵Pt{¹H} NMR (THF-*d*₈, 298 K): δ −3591 (broad d, ¹J_{P,Pt} = 2904 Hz).

Synthesis of 10. Complex **10** was prepared using the same procedure as for **3**, starting from Na[W(CO)₃Cp]·2DME (166 mg, 0.31 mmol) and **2** (110 mg, 0.14 mmol). Yield: 34%. Anal. Calcd for C₄₈H₄₁NO₅P₂PtSW₂: C 42.12, H 3.02, N 1.02; Found: C 42.24, H 3.08, N 0.99%. HRMS(+) in DME/MeOH (collision energy = 10 eV), exact mass for the cation [C₄₀H₃₆NO₂P₂PtSW]⁺ 1034.1080; measured: m/z : 1034.1094 [M−{W(CO)₃Cp}]⁺. HRMS(+) in DME/MeOH

(collision energy = 2 eV), exact mass for the cation $[C_{48}H_{41}NO_3P_2PtSW_2]^+$: 1369.0862 Da; measured m/z : 1369.0816 $[M]^+$. IR ν_{CO} (KBr)/ cm^{-1} : 1781 (vs), 1796 (vs), 1863 (vs), 1893 (vs), 1955 (vs), 1964 (vs); ν_{CO} (THF)/ cm^{-1} : 1787 (vs), 1885 (vs), 1966 (vs). 1H NMR (THF- d_6 , 298 K): δ 8.47 (dd, $^3J_{H,P} = 11$ Hz, $^3J_{H,H} = 8$ Hz, 2H, ortho- H_{ringB}), 7.92 (dd, $^3J_{H,P} = 11$ Hz, $^3J_{H,H} = 7$ Hz, 2H, ortho- H_{ringC}), 7.56 (overlapped, 2H, meta- H_{ringC}), 7.55 (overlapped, 2H, ortho- H_{ringD}), 7.47 (overlapped, 5H, para- H_{ringC} + ortho- H_{ringA} + meta- H_{ringD}), 7.41 (overlapped, 3H, para- H_{ringD} + meta- H_{ringB}), 7.29 (t, $^3J_{H,H} = 7$, 1 H, para- H_{ringB}), 7.08 (m, 3H, meta + para- $H_{benzyl\ ring}$), 6.97 (m, 2H, ortho- $H_{benzyl\ ring}$), 6.81 (very broad, 2H, meta- H_{ringA}), 6.65 (t, $^3J_{H,H} = 7$ Hz, 1H, para- H_{ringA}), 4.91 (s, 5 H, Cp- W^1), 4.79 (s, 5 H, Cp- W^2), $^2J_{H,H} = 14$ Hz, 1 H, C_6H_5HCH-S), 3.34 (d, $^2J_{H,H} = 14$ Hz, C_6H_5HCH-S), 3.15 (m, 1H, HCH-N), 2.90 (m, 1H, HCH-N), 1.99 (m, 1H, S-HCHCH $_2$ N), 1.83 (m, 2H, S-HCHCH $_2$ N). $^{13}C\{^1H\}$ APT (THF- d_6 , 298 K): δ 231.6 (d, $J_{C,P} = 21$ Hz, CO), 230.8 (d, $J_{C,P} = 21$ Hz, CO), 229.1 (br, CO), 227.9 (br, CO), 226.9 (br, CO), 144.2 (d, br, $J_{C,P} = 8$ Hz, C_{ipso}), 142.7 (d, br, $J_{C,P} = 6$ Hz, C_{ipso}), 138.2 (d, $J_{C,P} = 44$ Hz, C_{ipso}), 137.0 (s, C_{ipso}), 135.3 (d, $J_{C,P} = 14$ Hz, C_{ph}), 133.3 (d, $J_{C,P} = 51$ Hz, C_{ipso}), 133.0 (d, $J_{C,P} = 11$ Hz, C_{ph}), 132.6 (d, $J_{C,P} = 11$ Hz, C_{ph}), 132.5 (d, $J_{C,P} = 2$ Hz, C_{ph}), 132.3 (d, $J_{C,P} = 2$ Hz, C_{ph}), 130.9 (s, C_{ph}), 130.8 (d, $J_{C,P} = 2$ Hz, C_{ph}), 130.4 (d, $J_{C,P} = 10$ Hz, C_{ph}), 130.0 (d, $J_{C,P} = 10$ Hz, C_{ph}), 129.8 (m, C_{ph}), 129.2 (s, C_{ph}), 129.1 (s, C_{ph}), 128.9 (s, C_{ph}), 122.8 (s, C, benzyl ring), 92.8 (s, C_{Cp-W_2}), 90.8 (s, C_{Cp-W_1}), 48.4 (s, CH_2N), 39.9 (s, $PhCH_2S$), 26.9 (s, SCH_2CH_2N). $^{31}P\{^1H\}$ NMR (THF- d_6 , 298 K): δ 60.0 (d, $^2J_{P,P} = 55$ Hz, $^1J_{P,Pt} = 2875$ Hz, $^1J_{P,W} = 156$ Hz, P^1), 41.5 (d, $^2J_{P,P} = 55$ Hz, $^1J_{P,W} = 230$ Hz, $^3J_{P,Pt} = 20$ Hz, P^2). $^{195}Pt\{^1H\}$ NMR (THF, 298 K): δ -3605 (d, $^1J_{P,Pt} = 2875$ Hz).

Synthesis of Complexes 21–24. Solid $[n-Bu_4N]Cl$ (11 mg, 0.041 mmol) was added at room temperature to a stirred solution of **4** (46 mg, 0.041 mmol) in THF (3.0 mL). After it was stirred for 30 min, the brown solution turned dark red. To oxidize $[n-Bu_4N][Mo(CO)_3Cp]$, pure dioxygen (10 mL, 298 K, 1 atm) was bubbled into the solution through a gas-tight syringe causing, after further 30 min of stirring, the formation of a red suspension. The solvent was removed under reduced pressure, and the residue was treated with a 1:1 mixture of toluene and *n*-hexane (2.0 mL + 2.0 mL) five times; these fractions were collected. The yellow toluene/*n*-hexane solution was evaporated to dryness, and crystallization from THF/hexane yielded pure **22** as a yellow solid. Yield 57%. Anal. Calcd for $C_{40}H_{36}ClMoNO_2P_2PtS$ C 48.86, H 3.69, Cl 3.61, N 1.42; Found: C 48.78, H 3.60, Cl 3.54, N 1.36%. HRMS(+) in MeOH/HCOOH, exact mass for the cation $[C_{40}H_{36}ClKMoNO_2P_2PtS]^+$ 1021.9959; measured: m/z : 1021.9950 $[M+K]^+$. The spectrogram showed also an intense peak due to $[M-Cl]^+$ (experimental 948.0622 Da, calculated 948.0641 Da) and a peak due to the $[2M-Cl]^+$ (exp. 1931.0962 Da, calculated 1931.0979 Da). IR ν_{CO} (Nujol)/ cm^{-1} : 1965 (vs), 1893 (vs); ν_{Pt-Cl} (Nujol)/ cm^{-1} : 280 (m). 1H NMR ($CDCl_3$, 298 K): δ 8.55 (ddd, $^3J_{H,P} = 11$ Hz, $^3J_{H,H} = 8$ Hz, $^4J_{H,H} = 1$ Hz, 2H, ortho- H_{ringB}), 7.76 (ddd, $^3J_{H,P} = 11$ Hz, $^3J_{H,H} = 8$ Hz, $^4J_{H,H} = 1$ Hz, 2H, ortho- H_{ringC}), from 7.64 to 7.47 (m, 10 H, ortho- H_{ringD} + meta- H_{ringC} + meta- H_{ringD} + para- H_{ringC} + para- H_{ringD} + meta- H_{ringA}), 7.44 (m, 3H, meta- H_{ringB} + para- H_{ringB}), 7.22 (m, 5 $H_{benzyl\ ring}$), 6.96 (m, 3H, ortho- H_{ringA} + para- H_{ringA}), 4.74 (s, 5 H, Cp- Mo^1), 4.57 (d, $^2J_{H,H} = 14$ Hz, 1 H, C_6H_5HCH-S), 4.10 (d, $^2J_{H,H} = 14$ Hz, C_6H_5HCH-S), 3.04 (m, 1H, HCH-N), 2.79 (m, 1H, HCH-N), 1.94 (m, 2H, S- CH_2CH_2N). $^{13}C\{^1H\}$ APT ($CDCl_3$, 298 K): δ 243.4 (d, $J_{C,P} = 28$ Hz, CO), 239.6 (d, $J_{C,P} = 31$ Hz, CO), 142.6 (d, $J_{C,P} = 9$ Hz, C_{ipso}), 141.1 (d, $J_{C,P} = 3$ Hz, C_{ipso}), 139.7 (dd, $J_{C,P} = 12$ Hz, $J_{C,P} = 8$ Hz, C_{ipso}), 138.6 (s, C_{ph}), 137.7 (d, $J_{C,P} = 40$ Hz, C_{ipso}), 135.9 (d, $J_{C,P} = 12$ Hz, C_{ph}), 135.3 (s, C_{ipso}), 131.7 (d, $J_{C,P} = 11$ Hz, C_{ipso}), 131.4 (d, $J_{C,P} = 5$ Hz, C_{ph}), 131.0 (d, $J_{C,P} = 12$ Hz, C_{ph}), 130.4 (s, C_{ph}), 129.9 (s, C_{ph}), 129.3 (d, $J_{C,P} = 10$ Hz, C_{ph}), 128.7 (s, C_{ph}), 128.6 (d, $J_{C,P} = 25$ Hz, C_{ph}), 128.1 (m, C_{ph}), 127.9 (s, C_{ph}), 127.6 (s, C_{ph}), 127.0 (s, C_{ph}), 123.1 (s, C_{ph}), 94.4 (s, C_{Cp-Mo}), 46.5 (s, CH_2N), 39.9 (s, $PhCH_2S$), 24.1 (s, SCH_2CH_2N). $^{31}P\{^1H\}$ NMR ($CDCl_3$, 298 K): δ 75.8 (d, $^2J_{P,P} = 75$ Hz, $^1J_{P,Pt} = 3642$ Hz, P^1), 75.5 (d, $^2J_{P,P} = 75$ Hz, P^2). $^{195}Pt\{^1H\}$ NMR ($CDCl_3$, 298 K): δ -4034 (d, $^1J_{P,Pt} = 3642$ Hz).

Reactions of 3, 9, and 10 with $[n-Bu_4N]Cl$. The reactions between **3**, **9**, **10** and $[n-Bu_4N]Cl$ were performed in an NMR tube by mixing ca. 20 mg of trinuclear starting material with equimolar amounts of solid $[n-Bu_4N]Cl$ in 0.5 mL THF, using a D_2O capillary for lock, at 298 K.

In all cases, ^{31}P NMR analyses (Table 3) showed, after 20 min, the quantitative formation of the complexes **21**, **23**, and **24**.

Synthesis of 25. Complex **25** was prepared using the same procedure followed for **22**, starting from **4** (22 mg, 0.019 mmol) and solid $[n-Bu_4N]Br$ (6.26 mg, 0.019 mmol). Yield: 60%. Anal. Calcd for $C_{40}H_{36}BrMoNO_2P_2PtS$: C, 46.75; H, 3.53; N, 1.36; Found: C 46.28, H 3.40, N 1.34%. HRMS(+) in MeOH/HCOOH, exact mass for the cation $[C_{40}H_{36}BrKMoNO_2P_2PtS]^+$ 1049.9712; measured: m/z : 1049.9718 $[M+K]^+$. The spectrogram showed also an intense peak due to $[M-Br]^+$ (exp. 948.0636 Da, calculated 948.0641 Da). IR ν_{CO} (KBr)/ cm^{-1} : 1967 (vs), 1894 (vs). 1H NMR (C_6D_6 , 298 K): δ 8.72 (ddd, $^3J_{H,P} = 11$ Hz, $^3J_{H,H} = 8$ Hz, $^4J_{H,H} = 1$ Hz, 2 H, ortho- H_{ringB}), 8.24 (d, $^3J_{H,H} = 7$ Hz, $^4J_{H,H} = 1$ Hz, $^4J_{H,Pt} = 58$ Hz, 2 H, ortho- H_{ringA}), 7.64 (m, ortho- H_{ringC}), 7.40 (dd, $^3J_{H,P} = 11$ Hz, $^3J_{H,H} = 8$ Hz, 2 H, ortho- H_{ringD}), from 7.26 to 7.05 (m, 12 H, meta- H_{ringD} + meta- H_{ringA} + meta- H_{ringB} + para- H_{ringB} + para- H_{ringD} + para- H_{ringC} + ortho- $H_{benzyl\ ring}$ + para- $H_{benzyl\ ring}$), from 7.04 to 6.94 (m, 5 H, meta- H_{ringC} + meta- $H_{benzyl\ ring}$ + para- H_{ringA}), 4.90 (d, $^2J_{H,H} = 14$ Hz, 1 H, C_6H_5HCH-S), 4.55 (s, 5 H, Cp- Mo^1), 4.20 (d, $^2J_{H,H} = 14$ Hz, 1 H, C_6H_5HCH-S), 2.47 (m, 1 H, HCH-N), 2.40 (m, 1 H, HCH-N), 1.58 (m, 1 H, S-HCHCH $_2$ N), 1.46 (m, 1 H, S-HCHCH $_2$ N). $^{13}C\{^1H\}$ APT (C_6D_6 , 298 K): δ 244.1 (d, $J_{C,P} = 26$ Hz, CO), 239.9 (d, $J_{C,P} = 27$ Hz, CO), 142.8 (d, $J_{C,P} = 9$ Hz, C_{ipso}), 140.8 (d, $J_{C,P} = 14$ Hz, C_{ipso}), 140.1 (d, $J_{C,P} = 4$ Hz, C_{ph}), 137.9 (d, $J_{C,P} = 38$ Hz, C_{ipso}), 136.0 (s, C_{ipso}), 135.7 (d, $J_{C,P} = 12$ Hz, C_{ph}), 131.7 (d, $J_{C,P} = 44$ Hz, C_{ipso}), 131.6 (d, $J_{C,P} = 10$ Hz, C_{ph}), 130.9 (d, $J_{C,P} = 14$ Hz, C_{ph}), 130.7 (d, $J_{C,P} = 12$ Hz, C_{ph}), 130.1 (s, C_{ph}), 129.9 (s, C_{ph}), 128.9 (d, $J_{C,P} = 10$ Hz, C_{ph}), 128.6 (s, C_{ph}), 128.5 (s, C_{ph}), 128.4 (d, $J_{C,P} = 9$ Hz, C_{ph}), 128.0 (s, C_{ph}), 127.6 (s, C_{ph}), 126.9 (s, C_{ph}), 122.9 (s, C_{ph}), 94.3 (s, C_{Cp-Mo}), 46.4 (s, CH_2N), 41.3 (s, $PhCH_2S$), 23.9 (s, SCH_2CH_2N). $^{31}P\{^1H\}$ NMR (C_6D_6 , 298 K): δ 76.6 (d, $^2J_{P,P} = 74$ Hz, $^1J_{P,Pt} = 3560$ Hz, P^1), 74.8 (d, $^2J_{P,P} = 74$ Hz, P^2). $^{195}Pt\{^1H\}$ NMR (C_6D_6 , 298 K): δ -4110 (d, $^1J_{P,Pt} = 3560$ Hz).

Synthesis of 26. Complex **26** was prepared using the same procedure as followed for **22**, starting from **4** (22 mg, 0.019 mmol) and solid $[n-Bu_4N]I$ (7 mg, 0.019 mmol). Yield: 63%. Anal. Calcd for $C_{40}H_{36}IMoNO_2P_2PtS$: C, 44.70; H, 3.38; N, 1.30; Found: C 44.38, H 3.20, N 1.33%. HRMS(+) in MeOH/HCOOH, exact mass for the cation $[C_{40}H_{36}IKMoNO_2P_2PtS]^+$ 1097.9583; measured: m/z : 1097.9584 $[M+K]^+$. The spectrogram showed also an intense peak due to $[M-I]^+$ (exp. 948.0640 Da, calculated 948.0641 Da). IR ν_{CO} (Nujol)/ cm^{-1} : 1966 (vs), 1892 (vs). 1H NMR (C_6D_6 , 298 K): δ 8.76 (ddd, $^3J_{H,P} = 11$ Hz, $^3J_{H,H} = 7$ Hz, $^4J_{H,H} = 1$ Hz, 2 H, ortho- H_{ringB}), 8.29 (d, $^3J_{H,H} = 7$ Hz, $^4J_{H,H} = 1$ Hz, $^4J_{H,Pt} = 67$ Hz, 2 H, ortho- H_{ringA}), δ 7.70 (m, ortho- H_{ringC}), 7.36 (ddd, $^3J_{H,P} = 12$ Hz, $^3J_{H,H} = 7$ Hz, $^4J_{H,H} = 1$ Hz, 2 H, ortho- H_{ringD}), from 7.26 to 7.04 (m, 10 H, meta- H_{ringD} + meta- H_{ringA} + meta- H_{ringB} + para- H_{ringB} + para- H_{ringD} + ortho- $H_{benzyl\ ring}$), 6.99 (m, 4 H, meta- H_{ringC} + para- H_{ringC} + para- $H_{benzyl\ ring}$), 6.94 (m, 3 H, meta- $H_{benzyl\ ring}$ + para- H_{ringA}), 5.02 (d, $^2J_{H,H} = 14$ Hz, 1 H, C_6H_5HCH-S), 4.56 (s, 5 H, Cp- Mo^1), 3.96 (d, $^2J_{H,H} = 14$ Hz, 1 H, C_6H_5HCH-S), 2.63 (m, 1 H, HCH-N), 2.55 (m, 1 H, HCH-N), 1.40 (m, 2 H, S- CH_2CH_2N). $^{13}C\{^1H\}$ APT (C_6D_6 , 298 K): δ 243.4 (m, CO), 239.7 (m, CO), 141.9 (d, $J_{C,P} = 7$ Hz, C_{ipso}), 141.8 (d, br, $J_{C,P} = 7$ Hz, C_{ipso}), 137.6 (d, $J_{C,P} = 38$ Hz, C_{ipso}), 136.2 (s, C_{ipso}), 135.5 (m, C_{ph}), 131.6 (m, C_{ipso}), 131.3 (d, $J_{C,P} = 11$ Hz, C_{ph}), 131.2 (broad, C_{ph}), 131.0 (d, $J_{C,P} = 10$ Hz, C_{ph}), 130.9 (d, $J_{C,P} = 2$ Hz, C_{ph}), 130.8 (s, C_{ph}), 130.1 (s, C_{ph}), 129.7 (s, C_{ph}), 128.9 (m, C_{ph}), 128.6 (d, $J_{C,P} = 6$ Hz, C_{ph}), 128.5 (s, C_{ph}), 128.0 (s, C_{ph}), 127.6 (s, C_{ph}), 126.9 (s, C_{ph}), 122.7 (s, C_{ph}), 93.9 (s, C_{Cp-Mo}), 45.8 (s, CH_2N), 41.9 (s, $PhCH_2S$), 20.9 (s, SCH_2CH_2N). $^{31}P\{^1H\}$ NMR (C_6D_6 , 298 K): δ 75.0 (d, $^2J_{P,P} = 72$ Hz, $^1J_{P,Pt} = 3392$ Hz, P^1), 75.0 (d, $^2J_{P,P} = 72$ Hz, P^2). $^{195}Pt\{^1H\}$ NMR (C_6D_6 , 298 K): δ -4297 (d, $^1J_{P,Pt} = 3392$ Hz).

Reaction of 4 with I_2 . A round flask equipped with a dropping funnel containing a THF (1.0 mL) solution of I_2 (22 mg, 0.088 mmol) was charged with a brown THF solution of **4** (50 mg, 0.044 mmol in 2.0 mL) and placed under 1 atm of CO by means of a manifold. The I_2 solution was then dropped into the solution, and the mixture was stirred for 4 h at 298 K. The IR analysis of the resulting mixture showed, in the carbonyl region, very strong bands at 2040, 1974, 1963, and 1903 cm^{-1} , the first three ones being ascribed to $[MoI(CO)_3Cp]$.⁶⁹ The reaction solution was evaporated to dryness, and the residue was extracted with

C₆D₆ to give a dark solution submitted to multinuclear NMR analysis, revealing the formation of a 27/28 mixture in a 4/1 molar ratio.

Monitoring of the Reaction between 4 and Iodine. A J-valve NMR tube capped with a rubber septum containing a D₂O capillary was charged with a THF solution (0.3 mL) of 4 (22 mg, 0.017 mmol). The solution was placed under a CO atmosphere by using a CO/vacuum manifold, immersing the tube in an ice bath, and the dinitrogen atmosphere was replaced with pure CO. Thus, a THF solution (0.2 mL) of I₂ (9 mg, 0.034 mmol) was added with the aid of a syringe, and the tube was vigorously shaken. The resulting solution was submitted to ³¹P{¹H} NMR analysis, at 298 K, after 20 min, 1 h, and 2 h.

Synthesis of 27. To a THF solution (2 mL) of 26 (24 mg, 0.021 mmol), solid I₂ was added (5.0 mg, 0.021 mmol) with stirring at 298 K. After 1 h, the solvent was removed under reduced pressure, and 27 was obtained as a yellow solid by crystallization from THF/*n*-hexane. Anal. Calcd for C₃₄H₃₁I₂MoNO₂P₂PtS: C, 36.32; H, 2.78; N, 1.25; Found: C 36.25, H 2.70, N 1.21%. HRMS(+) in MeOH/HCOOH, exact mass for the cation [C₃₄H₃₁I₂KMoNO₂P₂PtS]⁺ 1163.7973; measured: *m/z*: 1163.7962; [M+K]⁺. The spectrogram showed also an intense peak due to [M-I]⁺ (exp. 997.9291 Da, calculated 997.9292 Da). IR ν_{CO} (CHCl₃)/cm⁻¹: 1982 (vs), 1911 (vs). ¹H NMR (C₆D₆, 298 K): δ 8.31 (ddd, ³J_{H,P} = 11 Hz, ³J_{H,H} = 8 Hz, ⁴J_{H,H} = 1 Hz, 2 H, ortho-H_{ringB}), 7.56 (dd, ³J_{H,P} = 11 Hz, ³J_{H,H} = 8 Hz, ortho-H_{ringC}), 7.45 (d, ³J_{H,H} = 7 Hz, 2 H, ortho-H_{benzyl ring}), 7.35 (ddd, ³J_{H,P} = 11 Hz, ³J_{H,H} = 8 Hz, ⁴J_{H,H} = 1 Hz, 2 H, ortho-H_{ringD}), 7.24 (pseudo t, ³J_{H,H} = 8 Hz, 2 H, meta-H_{ringC}), 7.11 (m, 2 H, meta-H_{ringB}) from 7.20 to 6.91 (m, 5 H, meta-H_{ringD} + para-H_{ringB} + para-H_{ringC} + para-H_{ringD}) 6.86 (t, ³J_{H,H} = 7 Hz, 1 H, para-H_{benzyl ring}), 6.61 (t, ³J_{H,H} = 7 Hz, 2 H, meta-H_{benzyl ring}), 4.49 (d, ²J_{H,H} = 14 Hz, 1 H, C₆H₅HCH-S), 5.15 (s, 5 H, Cp-Mo^I), 4.03 (d, ²J_{H,H} = 14 Hz, 1 H, C₆H₅HCH-S), 2.59 (m, 1 H, HCH-N), 2.46 (m, 1 H, HCH-N), 1.60 (m, 2 H, S-CH₂CH₂N). ¹³C{¹H} APT (C₆D₆, 298 K): δ 243.8 (d, J_{C,P} = 25 Hz, CO), 239.8 (d, J_{C,P} = 28 Hz, CO), from 139.0 to 124.0 (m, 16 C_{Ph}), 96.8 (s, C_{Cp-Mo}), 46.8 (s, CH₂N), 34.1 (s, PhCH₂S), 30.8 (s, SCH₂CH₂N). ³¹P{¹H} NMR (THF, 298 K): δ 65.1 (d, ²J_{P,P} = 74 Hz, ¹J_{P,Pt} = 2650 Hz, P^I), 77.8 (d, ²J_{P,P} = 74 Hz, P²). ¹⁹⁵Pt{¹H} NMR (THF, 298 K): δ -3343 (d, ¹J_{P,Pt} = 2650 Hz).

Synthesis of 28. A THF solution (2 mL) of (Ph₂P)₂N-(CH₂)₂SCH₂Ph (20 mg, 0.036 mmol) was added dropwise with stirring at 298 K within 30 min to a THF solution (2 mL) of [PtI₂(cod)] (20 mg, 0.036 mmol). After 30 min, the solution was concentrated (to ca. 0.5 mL), and the product was obtained by precipitation with *n*-hexane (10 mL). The pale yellow solid was washed with *n*-hexane (3 × 5 mL) and dried under vacuum. Yield: 92%. Anal. Calcd for C₃₃H₃₁Cl₂NP₂PtS: C, 49.44; H, 3.90; Cl, 8.85; N, 1.75; Found: C 49.37, H 3.83, Cl 8.79, N 1.72%. HRMS(+) in MeOH/HCOOH, exact mass for the cation [C₃₃H₃₁I₂NNaP₂PtS]⁺ 1006.9288; measured: *m/z*: 1006.9285 [M + Na]⁺. IR (nujol), ν /cm⁻¹: 3046 (m), 2932 (m), 1433 (s), 1313 (w), 1300 (w), 1159 (m), 1102 (vs), 1070 (m), 1026 (m), 1018 (m), 999 (m), 877 (s), 848 (s), 747 (s), 722 (s), 708 (w), 693 (vs), 664 (s), 576 (s), 518 (vs), 508 (vs), 491 (m), 473 (m), 438 (w), 407 (w), 381 (w), 296 (w). ¹H NMR (CDCl₃, 298 K): δ 7.76 (ddd, ³J_{H,P} = 12 Hz, ³J_{H,H} = 7 Hz, ⁴J_{H,H} = 2 Hz, 8 H, ortho-H_{Ph}), 7.65 (t, ³J_{H,H} = 7 Hz, 4 H, para-H_{Ph}), 7.52 (pseudo t, 8 H, meta-H_{Ph}) from 7.21 to 7.10 (m, 3 H, ortho-Bzyl + para-Bzyl), 6.93 (td, ³J_{H,H} = 7 Hz, ⁴J_{H,H} = 1 Hz, 2 H meta-Bzyl), 3.38 (s, 2 H, C₆H₅CH₂-S) 2.83 (m, 2 H, CH₂-N), 1.97 (m, 2 H, S-CH₂CH₂N). ¹³C{¹H} APT (CDCl₃, 298 K): δ 137.7 (s, C₆H₅CH₂-S, C_{ipso}), 133.8 (s, C_{para-Ph}), 133.5 (m, C_{ortho-Ph}) 129.8 (d, ³J_{C,P} = 13 Hz, C_{meta-Ph}) 128.9 (s, C_{ortho-Bzyl}) 128.8 (s, C_{meta-Bzyl}), 127.7 (m, C_{ipso}), 127.6 (s, C_{para-Bzyl}) 49.5 (s, ²J_{C,P} = 9 Hz, CH₂N), 36.5 (s, PhCH₂S), 29.0 (s, SCH₂CH₂N). ³¹P{¹H} NMR (C₆D₆, 298 K): δ 13.9 (d, ¹J_{P,Pt} = 3039 Hz). ¹⁹⁵Pt{¹H} NMR (THF, 298 K): δ -3457 (d, ¹J_{P,Pt} = 3010 Hz).

Reaction of 4 with Gaseous HCl. A Schlenk tube capped with a rubber septum was charged at 298 K with a THF solution (2.0 mL) of 4 (26 mg, 0.022 mmol) and placed under CO atmosphere by using a CO/vacuum manifold. Then, gaseous HCl (5.0 mL, 298 K, 1 atm) was bubbled into the THF solution by means of a gas-tight syringe. After a few minutes, the color of the solution turned from brown to orange. The reaction mixture was further stirred for 15 h, then submitted to multinuclear NMR analysis, which revealed the formation of a 2/29

mixture in a 4/1 molar ratio. The reaction of 4 with HCl(g) was monitored using a J-valve NMR tube capped with a rubber septum containing a D₂O capillary. The tube was charged with a THF solution (0.5 mL) of 4 (22 mg, 0.017 mmol), put under 1 atm of CO, and gaseous HCl was added (5.0 mL, 298 K, 1 atm), which was bubbled into the solution with the aid of a gas-tight syringe. The resulting solution was analyzed by ³¹P{¹H} NMR after 20 min, 6 h, 8 h, and 20 h, giving the following percentage ratios (n/a indicates not applicable):

time	2	22	29
20 min	20	80	n/a
6 h	20	53	27
8 h	20	45	35
20 h	20	n/a	80

Synthesis of 29. Gaseous HCl (5.0 mL, 298 K, 1 atm) was bubbled into a vigorously stirred THF solution (2 mL) of 22 (26 mg, 0.022 mmol) at 298 K causing a color change of the solution from brown to orange. After 20 min the solution was concentrated to 0.5 mL, and the product was obtained as a yellow solid by precipitation with *n*-hexane. The solid was washed with *n*-hexane (3 × 5 mL) and dried under vacuum. Yield: 83%. Anal. Calcd for C₃₄H₃₁Cl₂MoNO₂P₂PtS: C, 43.37; H, 3.32; Cl, 7.53; N, 1.49; Found: C, 43.10; H, 3.28, Cl, 7.41; N, 1.46%. HRMS(+) in MeOH/HCOOH, exact mass for the cation [C₃₄H₃₁Cl₂KMoNO₂P₂PtS]⁺ 979.9246; measured: *m/z*: 979.9251 [M+K]⁺. The spectrogram showed also an intense peak due to [M-Cl]⁺ (exp. 905.9957 Da, calculated 905.9930 Da). IR ν_{CO} (Nujol)/cm⁻¹: 1970 (vs), 1899 (vs); $\nu_{\text{Pt-Cl}}$ (Nujol)/cm⁻¹: 331 (s) 269 (m). ¹H NMR (CDCl₃, 298 K): δ 7.87 (ddd, ³J_{H,P} = 11 Hz, ³J_{H,H} = 8 Hz, ⁴J_{H,H} = 1 Hz, 2 H, ortho-H_{ringB}), from 7.67 to 7.50 (m, 10 H, ortho-H_{ringC}, ortho-H_{ringD}, meta-H_{ringC}, meta-H_{ringD}, para-H_{ringC}, para-H_{ringD}) from 7.34 to 7.19 (m, 3 H, meta-H_{ringB}, para-H_{ringB}), 5.45 (s, 5 H, Cp-Mo), 4.98 (d, ²J_{H,H} = 13 Hz, 1 H, C₆H₅HCH-S), 4.16 (d, ²J_{H,H} = 13 Hz, 1 H, C₆H₅HCH-S), 2.99 (m, 1 H, HCH-N), 2.48 (m, 1 H, HCH-N), 1.95 (m, 1 H, S-HCHCH₂N), 1.59 (m, 1 H, S-HCHCH₂N). ¹³C{¹H} APT (CDCl₃, 298 K): δ 241.8 (d, J_{C,P} = 30 Hz, CO), 235.3 (d, J_{C,P} = 28 Hz, CO), 139.0 (m, C_{ipso}), 137.6 (d, J_{C,P} = 4 Hz, C_{Ph}), 137.5 (d, J_{C,P} = 35 Hz, C_{ipso}), 137.0 (s, C_{ipso}), 135.7 (d, J_{C,P} = 41 Hz, C_{ipso}), 130.8 (m, overlapped, C_{Ph}), 130.7 (m, overlapped, C_{Ph}), 129.6 (s, C_{Ph}), 129.0 (s, C_{Ph}), 128.3 (d, J_{C,P} = 11 Hz, C_{Ph}), 128.2 (s, C_{Ph}), 127.8 (s, C_{Ph}), 127.5 (s, C_{Ph}), 127.4 (d, J_{C,P} = 12 Hz, C_{Ph}), 127.0 (s, C_{Ph}), 124.5 (s, C_{Ph}), 94.5 (s, C_{Cp-Mo}), 46.7 (s, CH₂N), 31.2 (broad, PhCH₂S), 28.9 (broad, SCH₂CH₂N). ³¹P{¹H} NMR (CDCl₃, 298 K): δ 63.8 (d, ²J_{P,P} = 82 Hz, ¹J_{P,Pt} = 2971 Hz, P^I), 81.6 (d, ²J_{P,P} = 82 Hz, P²). ¹⁹⁵Pt{¹H} NMR (CDCl₃, 298 K): δ -3793 (d, ¹J_{P,Pt} = 2971 Hz).

Monitoring of the Reaction between 1 and Na[Mo(CO)₃Cp]-2DME. To a Schlenk tube containing a stirred THF solution (2.0 mL) of 1 (60 mg, 0.053 mmol) at 323 K was added a solution of Na[Mo(CO)₃Cp]-2DME (52 mg, 0.117 mmol) in THF (22 mL) in successive portions of 10 mL (*t* = 0), 5 mL (after 1 h), and 7 mL (after two more hours), by means of a dropping funnel. Thirty minutes after each addition, an aliquot of the mixture (0.3 mL) was transferred into an NMR tube containing a D₂O capillary and used for recording ³¹P{¹H} NMR spectra at 298 K. The course of the reaction between 1 and Na[W(CO)₃Cp], or 2 and Na[Mo(CO)₃Cp], or 2 and Na[W(CO)₃Cp] was monitored in an analogous manner.

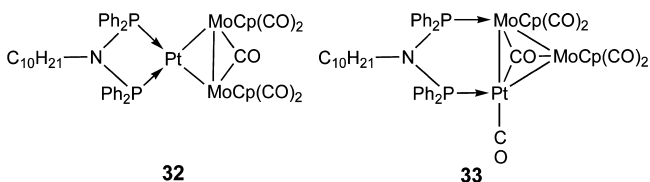
Monitoring of the Reaction Performed by Sequential Addition of Na[Mo(CO)₃Cp] and Na[W(CO)₃Cp] to 2. To a Schlenk tube containing a stirred THF solution (2.0 mL) of 2 (42 mg, 0.053 mmol) at 323 K was added first a solution of Na[Mo(CO)₃Cp]-2DME (24 mg, 0.053 mmol) in THF (1.0 mL) and then a solution of Na[W(CO)₃Cp]-2DME (28 mg, 0.053 mmol) in THF (1.0 mL) by means of dropping funnels kept under argon atmosphere.

In an analogous manner, to a THF solution (2.0 mL) of 1 (60 mg, 0.053 mmol) kept under stirring at 323 K, was added first a solution of Na[W(CO)₃Cp]-2DME (28 mg, 0.053 mmol) in THF (1.0 mL) and then a solution of Na[Mo(CO)₃Cp]-2DME (24 mg, 0.053 mmol) in THF (1.0 mL).

After each addition, an aliquot of the mixture (0.3 mL) was transferred into an NMR tube containing a D₂O capillary and used for recording ³¹P{¹H} and ¹⁹⁵Pt{¹H} NMR spectra at 298 K. Main spectroscopic

features of the mixed Pt–Mo–W species **30** and **31** are reported in Table 4

Reaction in the Presence of Di-*n*-butylsulfide. Neat di-*n*-butylsulfide (0.10 mL) was added to a vigorously stirred THF solution (2.0 mL) of complex $[\text{PtCl}_2\{(\text{Ph}_2\text{P})_2\text{N}(n\text{-decyl})\}]$ (60 mg, 0.076 mmol) kept at 323 K. Then, solid $\text{Na}[\text{Mo}(\text{CO})_3\text{Cp}]$ (69 mg, 0.152 mmol) was added to the solution and immediately the solution turned from colorless to brown. The multinuclear NMR analysis of the reaction solution revealed the formation of an 88/22 (mol/mol) mixture of the complexes **32** and **33**.³



Computational Details. All calculations were performed at DFT level by using Jaguar 7.5 program.⁷⁰ Geometry optimizations were performed by using the B3LYP and M06 exchange-correlation functionals.^{71–73}

For all considered complexes, an exhaustive search of the most stable structures—including possible isomers and conformers—was performed in gas phase using the B3LYP functional and an LACVP* basis set, consisting of the 6-31G(d) set for the main-group elements,⁷⁴ and the Hay and Wadt core valence ECP basis set of double- ζ quality plus one polarization f functions for the metal atoms.^{75–77} For the most stable structures of each complex, vibrational frequency calculations based on analytical second derivatives at the same level of theory were performed to confirm the nature of the local minima and transition state and to compute the zero-point-energy (ZPE) and vibrational entropy corrections at 298.15 K. These structures were then reoptimized in gas phase at the M06/LACVP* level of theory.

Solvation energies were evaluated by using the Poisson–Boltzmann continuum solvent method implemented in Jaguar to simulate the THF environment ($\epsilon = 24.3$ and $\sigma = 2.262 \text{ \AA}$).^{78,79} Solvation energies were only evaluated on the gas-phase stationary points. The electronic and solvation energies of all the most stable stationary points were reevaluated with single-point calculation using the larger LACVP++** basis set, consisting of the 6-311++G(d,p) set for the main-group elements⁸⁰ and the Hay and Wadt core valence ECP basis set of triple- ζ quality plus one diffuse d function and two polarization sp functions for all metal atoms.^{75–77} The reaction enthalpies in solution were estimated by adding the solvation free energy to the corresponding gas-phase enthalpy.

Although our approach—geometry optimizations in gas phase followed by single-point calculations in solvent and with a larger basis set—is standard in theoretical chemistry, optimization in solution that may give better results for systems involving ion pairs. However, the large size of the considered systems, up to almost 100 atoms and more than 1000 basis set functions, make optimization and especially frequency calculations in solution computationally far too demanding and practically unfeasible. To better investigate the possible errors due to this approximate approach, we considered the simplest prototype ion pair model involved in the considered systems, that is, $\text{Na}[\text{Mo}(\text{CO})_3\text{Cp}]$, by performing (i) a geometry optimization in gas phase followed by single-point calculations in solvent and with a larger basis set; (ii) a geometry optimization in solution followed by a single-point calculation with a larger basis set. The results show negligible geometry changes (except 0.7 Å for the $\text{Na}^+\cdots\text{O}$ distances) and a moderate energy relaxation of $\sim 6 \text{ kcal}\cdot\text{mol}^{-1}$, which is, however, expected to affect much less the energy differences involved in reaction and activation energies due to error compensation.

For the reaction involving the formation of solid NaCl, the absolute standard enthalpy, $H^\circ_{(\text{NaCl})}$, and Gibbs free energy, $G^\circ_{(\text{NaCl})}$, of the NaCl crystal were evaluated combining the calculated Na^+ and Cl^- gas-phase absolute standard enthalpies, $H^\circ_{(\text{Na}^+)}$ and $H^\circ_{(\text{Cl}^-)}$, and standard Gibbs free energies, $G^\circ_{(\text{Na}^+)}$ and $G^\circ_{(\text{Cl}^-)}$, with the experimental lattice energy,

$\Delta H^\circ_{(\text{lattice, exp})}$ and absolute standard entropies, $S^\circ_{(\text{exp})}$, of the crystal, according to

$$H^\circ_{(\text{NaCl})} = H^\circ_{(\text{Na}^+)} + H^\circ_{(\text{Cl}^-)} + \Delta H^\circ_{(\text{lattice, exp})}$$

$$G^\circ_{(\text{NaCl})} = H^\circ_{(\text{NaCl})} - TS^\circ_{(\text{exp})}$$

Although the B3LYP exchange correlation functional has been increasingly and successfully employed in DFT calculations in the last two decades, it does not adequately treat dispersion interactions, and it has recently emerged that it may give inaccurate geometries and energies when large molecules with significant steric and hydrophobic intramolecular interaction are considered. Recent benchmark studies have shown that a newly developed exchange-correlation functional explicitly built to take into account these effects, such as ML06, may give much better results.⁷³ In a previous study we performed benchmark calculations at both B3LYP and M06 levels on a series of PtCo_2 trinuclear cluster similar to those considered in this study,³ namely, $[\text{PtCo}_2(\text{CO})_7\{(\text{Ph}_2\text{P})_2\text{NR}\}]$ with $\text{R} = (\text{CH}_2)_9\text{CH}_3$, $(\text{CH}_2)_5\text{S}(\text{CH}_2)_5\text{CH}_3$, $(\text{CH}_2)_2\text{SCH}_2\text{C}_6\text{H}_5$, C_6H_5 , for which a large amount of experimental structural and thermodynamic data (on the equilibrium between the bridged and chelate isomers) are available, and found that only the M06 results were in reasonable agreement with the experimental data for the isomerization enthalpies and free energies.⁸ Moreover, this level of theory has been already successfully employed in theoretical studies of the PtMo_2 and PtW_2 cluster, giving results in good agreement with all experimental findings.³

■ ASSOCIATED CONTENT

Supporting Information

HRMS(+) spectrogram and NMR spectra of **3**, **4**, **9**, **10**; calculated geometries of **4**, **11**, and **12**; free energy profile for the formation of **15**, **7**, and **5**, **B–D**, and **3**; reaction courses of the reactions between **1** and $\text{Na}[\text{Mo}(\text{CO})_3\text{Cp}]$ or $\text{Na}[\text{W}(\text{CO})_3\text{Cp}]$; proposed mechanism for the reaction of **4** with HCl; Mulliken charges on selected atoms of the intermediates **B**, **E**, **F**, **G**, **H**, **I**, and of $\text{TS}_{\text{H–I}}$. Cartesian coordinates of **3**, **B**, **E**, **F**, **G**, **H**, **I**, $\text{TS}_{\text{F–G}}$, and $\text{TS}_{\text{H–I}}$ calculated at M06/LACVP* level. The Supporting Information is available free of charge on the ACS Publications website at DOI: 10.1021/acs.inorgchem.5b00223.

■ AUTHOR INFORMATION

Corresponding Authors

*E-mail: braunstein@unistra.fr. (P.B.)

*E-mail: pietro.mastorilli@poliba.it. (P.M.)

Notes

The authors declare no competing financial interest.

■ ACKNOWLEDGMENTS

We wish to thank the reviewers for their valuable suggestions. The Politecnico di Bari (FRA funds to M.L.), the CNRS, the MESR (Paris), and the Université de Strasbourg are gratefully acknowledged for financial support.

■ REFERENCES

- (1) Selected review articles: (a) Puddephatt, R. J. *Chem. Soc. Rev.* **1983**, *12*, 99–127. (b) Witt, M.; Roesky, H. W. *Chem. Rev.* **1994**, *94*, 1163–1181. (c) Balakrishna, M. S.; Sreenivasa Reddy, Y.; Krishnamurthy, S. S.; Nixon, J. F.; Burckett St. Laurent, J. C. T. R. *Coord. Chem. Rev.* **1994**, *129*, 1–254. (d) Mague, J. T. J. *Cluster Sci.* **1995**, *6*, 217. (e) Bhattacharyya, P.; Woollins, J. D. *Polyhedron* **1995**, *14*, 3367–3388. (f) Braunstein, P.; Knorr, M.; Stern, C. *Coord. Chem. Rev.* **1998**, *178–180*, 903–965. (g) Appleby, T.; Woollins, J. D. *Coord. Chem. Rev.* **2002**, *235*, 121–140.
- (2) See, for example, (a) Ghisolfi, A.; Fliedel, C.; Rosa, V.; Monakhov, K. Yu.; Braunstein, P. *Organometallics* **2014**, *33*, 2523–2534. (b) Fliedel, C.; Faramarzi, V.; Rosa, V.; Douidin, B.; Braunstein, P. *Chem.—Eur. J.* **2014**, *20*, 1263–1266. (c) Ghisolfi, A.; Fliedel, C.; Rosa, V.; Pattacini, R.;

- Thibon, A.; Monakhov, K. Yu.; Braunstein, P. *Chem.—Asian J.* **2013**, *8*, 1795–1805. (d) Rodriguez-Zubiri, M.; Gallo, V.; Rosé, J.; Welter, R.; Braunstein, P. *Chem. Commun.* **2008**, 64–66.
- (3) Todisco, S.; Gallo, V.; Mastrorilli, P.; Latronico, M.; Re, N.; Creati, F.; Braunstein, P. *Inorg. Chem.* **2012**, *51*, 11549–11561.
- (4) Braunstein, P.; Guarino, N.; de Méric de Bellefon, C.; Richert, J.-L. *Angew. Chem., Int. Ed. Engl.* **1987**, *26*, 88–89.
- (5) Bachert, I.; Bartussek, I.; Braunstein, P.; Guillon, E.; Rosé, J.; Kickelbick, G. *J. Organomet. Chem.* **1999**, *580*, 257–264.
- (6) Bachert, I.; Bartussek, I.; Braunstein, P.; Guillon, E.; Rosé, J.; Kickelbick, G. *J. Organomet. Chem.* **1999**, *588*, 144–151.
- (7) Braunstein, P.; de Méric de Bellefon, C.; Oswald, B. *Inorg. Chem.* **1993**, *32*, 1649–1655.
- (8) Gallo, V.; Mastrorilli, P.; Nobile, C. F.; Braunstein, P.; Englert, U. *Dalton Trans.* **2006**, 2342–2349.
- (9) Braunstein, P.; de Méric de Bellefon, C.; Lanfranchi, M.; Tiripicchio, A. *Organometallics* **1984**, *3*, 1772–1774.
- (10) Buchwalter, P.; Rosé, J.; Braunstein, P. *Chem. Rev.* **2015**, *115*, 28–126.
- (11) Siedle, A. R.; Newmark, R. A.; Gleason, W. B. *J. Am. Chem. Soc.* **1986**, *108*, 767–773.
- (12) Jans, J.; Naegeli, R.; Venanzi, L. M.; Albinati, A. *J. Organomet. Chem.* **1983**, *247*, C37–C41.
- (13) van Leeuwen, P. W. N. M.; Roobeek, C. F.; Orpen, A. G. *Organometallics* **1990**, *9*, 2179–2181.
- (14) (a) Taylor, N. J.; Chieh, P. C.; Carty, A. J. *J. Chem. Soc., Chem. Commun.* **1975**, 448–449. (b) Bender, R.; Braunstein, P.; Tiripicchio, A.; Tiripicchio-Camellini, M. *Angew. Chem., Int. Ed. Engl.* **1985**, *24*, 861–862. (c) Bender, R.; Braunstein, P.; Dedieu, A.; Ellis, P. D.; Huggins, B.; Harvey, P. D.; Sappa, E.; Tiripicchio, A. *Inorg. Chem.* **1996**, *35*, 1223–1234. (d) Bender, R.; Welter, R.; Braunstein, P. *Inorg. Chim. Acta* **2015**, *424*, 20–28.
- (15) The reaction led to a mixture of the corresponding chelate and bridged PtMo₂ isomers in an 11:1 ratio, as reported in ref 3.
- (16) Bender, R.; Braunstein, P.; Jud, J.-M.; Dusaouy, Y. *Inorg. Chem.* **1984**, *23*, 4489–4502.
- (17) Tsutsuminai, S.; Komine, N.; Hirano, M.; Komiya, S. *Organometallics* **2004**, *23*, 44–53.
- (18) Tsutsuminai, S.; Komine, N.; Hirano, M.; Komiya, S. *Organometallics* **2003**, *22*, 4238–4247.
- (19) Fukuoka, A.; Sadashima, T.; Endo, I.; Ohashi, N.; Kambara, Y.; Sugiura, T.; Komiya, S. *Organometallics* **1994**, *13*, 4033–4044.
- (20) Blum, T.; Braunstein, P. *Organometallics* **1989**, *8*, 2504–2513.
- (21) Komine, N.; Tsutsuminai, S.; Hoh, H.; Yasuda, T.; Hirano, M.; Komiya, S. *Inorg. Chim. Acta* **2006**, *359*, 3699–3708.
- (22) Knorr, M.; Strohmann, C. *Organometallics* **1999**, *18*, 248–257.
- (23) Mead, K. A.; Moore, I.; Stone, F. G. A.; Woodward, P. *J. Chem. Soc., Dalton Trans.* **1983**, 2083–2090.
- (24) Awang, M. R.; Jeffery, J. C.; Stone, F. G. A. *J. Chem. Soc., Dalton Trans.* **1983**, 2091–2098.
- (25) Awang, M. R.; Barr, R. D.; Green, M.; Howard, J. A. K.; Marder, T. B.; Stone, F. G. A. *J. Chem. Soc., Dalton Trans.* **1985**, 2009–2016.
- (26) Powell, J.; Sawyer, J. F.; Smith, S. J. *J. Chem. Soc., Chem. Commun.* **1985**, 1312–1313.
- (27) Lukehart, C. M.; True, W. R. *Organometallics* **1988**, *7*, 2387–2393.
- (28) Braunstein, P.; de Méric de Bellefon, C.; Oswald, B.; Ries, M.; Lanfranchi, M.; Tiripicchio, A. *Inorg. Chem.* **1993**, *32*, 1638–1648.
- (29) Browning, C. S.; Farrar, D. H. *J. Chem. Soc., Dalton Trans.* **1995**, 521–530.
- (30) The collision energy is the energy difference between quadrupole and collision cell applied at the exit of the quadrupole and contributes to accelerate the ions preformed in the ionization chamber to transfer them to the collision cell. In the present study a lower collision energy allowed the detection of labile ions.
- (31) Throughout the paper, the calculated (exact mass) and the experimental (accurate) *m/z* values were compared considering the principal ion (which gives the most intense peak) of the isotope pattern.
- (32) Curtis, M. D.; Han, K. R. *Inorg. Chem.* **1985**, *24*, 378–382.
- (33) Garrou, P. E. *Chem. Rev.* **1985**, *85*, 171–185.
- (34) Parkins, A. W. *Coord. Chem. Rev.* **2006**, *250*, 449–467.
- (35) Macgregor, S. A. *Chem. Soc. Rev.* **2007**, *36*, 67–76.
- (36) Geldbach, T. J.; Pregosin, P. S. *Eur. J. Inorg. Chem.* **2002**, 1907–1918.
- (37) Chakravarty, A. R.; Cotton, F. A.; Tocher, D. A. *J. Am. Chem. Soc.* **1984**, *106*, 6409–6413.
- (38) Vierling, P.; Riess, J. G. *J. Am. Chem. Soc.* **1981**, *103*, 2466–2467.
- (39) Nakazawa, H.; Matsuoka, Y.; Nakagawa, I.; Miyoshi, K. *Organometallics* **1992**, *11*, 1385–1392.
- (40) Mizuta, T.; Yamasaki, T.; Nakazawa, H.; Miyoshi, K. *Organometallics* **1996**, *15*, 1093–1100.
- (41) Liniger, M.; Gschwend; Neuburger, M.; Schaffner, S.; Pfaltz, A. *Organometallics* **2010**, *29*, 5953–5958.
- (42) Shaw, B. K.; Patrick, B. O.; Fryzuk, M. D. *Organometallics* **2012**, *31*, 783–786.
- (43) Ai, P.; Danopoulos, A. A.; Braunstein, P. *Dalton Trans.* **2014**, *43*, 1957–1960.
- (44) Fahey, D. R.; Mahan, J. E. *J. Am. Chem. Soc.* **1976**, *98*, 4499–4503.
- (45) Vierling, P.; Riess, J. G.; Grand, A. *Inorg. Chem.* **1986**, *25*, 4144–4152.
- (46) Cabeza, J. A.; del Rio, I.; Riera, V.; Garcia-Granda, S.; Sanni, S. B. *Organometallics* **1997**, *16*, 1743–1748.
- (47) Geldbach, T. J.; Pregosin, P. S.; Bassetti, M. *Organometallics* **2001**, *20*, 2990–2997.
- (48) Arias, A.; Forniés, J.; Fortuño, C.; Martín, A.; Latronico, M.; Mastrorilli, P.; Todisco, S.; Gallo, V. *Inorg. Chem.* **2012**, *51*, 12682–12696.
- (49) Archambault, C.; Bender, R.; Braunstein, P.; De Cian, A.; Fischer, J. *Chem. Commun.* **1996**, 2729–2730.
- (50) Chaouche, N.; Forniés, J.; Fortuño, C.; Kribii, A.; Martín, A.; Karipidis, P.; Tsipis, A. C.; Tsipis, C. A. *Organometallics* **2004**, *23*, 1797–1810.
- (51) Forniés, J.; Fortuño, C.; Ibáñez, S.; Martín, A. *Inorg. Chem.* **2006**, *45*, 4850–4858.
- (52) Ara, I.; Chaouche, N.; Forniés, J.; Fortuño, C.; Kribii, A.; Tsipis, A. C. *Organometallics* **2006**, *25*, 1084–1091.
- (53) The massive formation of PhI was detected by GC-MS analysis of the reaction solution after workup.
- (54) The reaction was performed either under N₂ or under CO giving the same outcome.
- (55) Piper, T. S.; Wilkinson, G. *J. Inorg. Nucl. Chem.* **1956**, *3*, 104–124.
- (56) The other carbonyl band at 1968 cm⁻¹ (with a shoulder at 1955 cm⁻¹) of [Mo(CO)₃Cp] overlaps with the carbonyl bands of **26** and **27**.
- (57) The formation of **28** might be imputed to the presence of CO deriving from little decomposition of **4** or **26** in solution.
- (58) Nakazawa, H.; Yamaguchi, Y.; Mizuta, T.; Ichimura, S.; Miyoshi, K. *Organometallics* **1995**, *14*, 4635–4643.
- (59) Kawamura, K.; Nakazawa, H.; Miyoshi, K. *Organometallics* **1999**, *18*, 4785–4794.
- (60) The reaction solution showed at the ³¹P NMR analysis signals ascribable to trinuclear bridged and chelate complexes having Pt-Mo-W cores.
- (61) The addition of *n*-Bu₄NCl to the mixture obtained after reaction showed at the ³¹P NMR the disappearing of the signals ascribed to **31** (and **4**), and the appearance of the signals due to **22** (δ 75.4 and δ 74.6), thus confirming the structure proposed for **31**.
- (62) In this case, the addition of *n*-Bu₄NCl to the mixture obtained after reaction showed in the ³¹P NMR the disappearing of the signals ascribed to **4**, **9**, **30**, and **31** and the appearance of the signals due to **22** and **24**.
- (63) Chatt, J.; Vallarino, L. M.; Venanzi, L. M. *J. Chem. Soc.* **1957**, 2496–2505.
- (64) Braunstein, P.; Bender, R.; Jud, J. *Inorg. Synth.* **1989**, *26*, 341–350.
- (65) Crystallographic data (excluding structure factors) for [4] and [9] were deposited with the Cambridge Crystallographic Data Centre as supplementary publication No. CCDC 1043480 [4] and CCDC 1043481 [9]. Copies of the data can be obtained free of charge on application to CCDC, 12 Union Road, Cambridge CB2 1EZ, U.K. [Fax:

international code + 44(1223)336-033; E-mail: deposit@ccdc.cam.ac.uk].

(66) Sheldrick, G. M. *SADABS*, Program for Empirical Absorption Correction of Area Detector Data; University of Göttingen: Göttingen, Germany, 1996.

(67) Sheldrick, G. M. *Acta Crystallogr., Sect. A* **2008**, *64*, 112–122.

(68) Hirshfeld, F. L. *Acta Crystallogr., Sect. A* **1976**, *32*, 239–244.

(69) Piper, T. S.; Wilkinson, G. J. *Inorg. Nucl. Chem.* **1956**, *3*, 104–124.

(70) *Jaguar*, Version 6.0; Schrödinger, LLC.: New York, NY, 2005.

(71) Becke, A. D. *J. Chem. Phys.* **1993**, *98*, 5648–5652.

(72) Lee, C. T.; Yang, W. T.; Parr, R. G. *Phys. Rev.* **1988**, *37*, 785–789.

(73) Zhao, Y.; Truhlar, D. G. *Theor. Chem. Acc.* **2008**, *120*, 215–241.

(74) Hehre, W. J.; Ditchfield, R.; Pople, J. A. *J. Chem. Phys.* **1972**, *56*, 2256–2261.

(75) Hay, P. J.; Wadt, W. R. *J. Chem. Phys.* **1985**, *82*, 270–283.

(76) Wadt, W. R.; Hay, P. J. *J. Chem. Phys.* **1985**, *82*, 284–298.

(77) Hay, P. J.; Wadt, W. R. *J. Chem. Phys.* **1985**, *82*, 299–310.

(78) Tomasi, J.; Persico, M. *Chem. Rev.* **1994**, *94*, 2027–2094.

(79) Cramer, C. J.; Truhlar, D. G. *Chem. Rev.* **1999**, *99*, 2161–2200.

(80) Krishnan, R.; Binkley, J. S.; Seeger, R.; Pople, J. A. *J. Chem. Phys.* **1980**, *72*, 650–654.

■ NOTE ADDED AFTER ASAP PUBLICATION

This paper was published on the Web on May 5, 2015, with the incorrect artwork for Scheme 4. The corrected version was reposted on May 6, 2015.